Image-guided Treatment in the Hepatobiliary System: Role of Imaging in Treatment Planning and Posttreatment Evaluation[1]

Surabhi Bajpai, DMRD
Avinash Kambadakone, MD, FRCR
Alexander R. Guimaraes, MD, PhD
Ronald S. Arellano, MD
Debra A. Gervais, MD
Dushyant Sahani, MD

Abbreviations: ADC = apparent diffusion coefficient, EASL = European Association for the Study of the Liver, FDG = fluorodeoxyglucose, HCC = hepatocellular carcinoma, IGRT = image-guided radiation treatment, mRECIST = Modified Response Evaluation Criteria in Solid Tumors, RECIST = Response Evaluation Criteria in Solid Tumors, RFA = radiofrequency ablation, SIRT = selective internal radiation therapy, TACE = transarterial chemoembolization

RadioGraphics 2015; 35:1393–1418

Published online 10.1148/rg.2015140281

Content Codes: CT GI MR NM OI

[1]From the Division of Abdominal Imaging, Massachusetts General Hospital, 55 Fruit St, White 270, Boston, MA 02114. Presented as an education exhibit at the 2013 RSNA Annual Meeting. Received August 23, 2014; revision requested December 10 and received January 26, 2015; accepted January 29. For this journal-based SA-CME activity, the authors A.R.G and D.S. have provided disclosures (see p 1416); all other authors, the editor, and the reviewers have disclosed no relevant relationships. **Address correspondence to** D.S. (e-mail: *dsahani@mgh.harvard.edu*).

SA-CME LEARNING OBJECTIVES

After completing this journal-based SA-CME activity, participants will be able to:

■ Discuss the principles of various image-guided therapies in management of hepatobiliary tumors.

■ Recognize the role of imaging in pretreatment planning to ensure optimal treatment delivery.

■ Describe the value of morphologic and functional imaging, including the role of advanced postprocessing methods, in posttreatment follow-up and monitoring of therapeutic response.

See www.rsna.org/education/search/RG.

In the past decade, image-guided targeted treatments such as percutaneous ablation, intra-arterial embolic therapies, and targeted radiation therapy have shown substantial promise in management of hepatobiliary malignancies. Imaging is integral to patient selection, treatment delivery, and assessment of treatment effectiveness. Preprocedural imaging is crucial and allows local tumor staging, evaluation of surrounding structures, and selection of suitable therapeutic options and strategies for treatment delivery. Postprocedural imaging is required to monitor therapeutic success, detect residual or recurrent disease, and identify procedure-related complications to guide appropriate future therapy. Technical innovations in cross-sectional imaging techniques such as computed tomography (CT) and magnetic resonance (MR) imaging, combined with advances in image postprocessing and new types of contrast agents, allow precise morphologic assessment and functional evaluation of hepatobiliary tumors. Advanced postprocessing techniques such as image fusion and volumetric assessment not only facilitate procedural planning and treatment delivery but also enhance posttreatment imaging surveillance. In addition, molecular imaging techniques such as fluorodeoxyglucose positron emission tomography (PET), PET/CT, and PET/MR imaging offer opportunities to evaluate various physiologic properties of tumors.

Introduction

In the current era of personalized medicine, several treatment strategies are available for management of hepatobiliary malignancies (1–5). Surgical resection is considered the criterion standard for management of resectable malignant tumors in the liver and biliary system in suitable candidates. In the past decade, organ-directed treatments such as percutaneous ablation, intra-arterial embolic therapy, and targeted radiation therapy have shown substantial promise in management of these tumors (Fig 1, Table 1) (6,16,21–23). While percutaneous ablative therapies offer a suitable alternative to surgical resection, intra-arterial embolic interventions are a mainstay in patients with more advanced local disease (6,11–13,16,21–24). IGRT is a valuable therapeutic option for patients with unresectable or hard-to-ablate hepatic malignancies (19,25).

TEACHING POINTS

- When percutaneous ablation is selected, tumor size has considerable influence on the treatment plan, including determination of the type and number of electrode probes (eg, single vs clustered probes). Tumor size is a strong predictor of treatment success and survival in patients with primary or metastatic liver malignancies, as demonstrated in several studies.
- In patients undergoing percutaneous ablation, precise delineation of tumor location helps determine the needle trajectory or path to the tumor and type of ablative technique selected (eg, RFA vs microwave ablation) and also influences other aspects of percutaneous treatment, such as patient positioning, type of electrode used, and need for adjunctive procedures (eg, hydrodissection).
- FDG PET/CT is superior to CT for detection of intra- and extrahepatic recurrences after local-regional therapies, particularly in hepatic metastases from extrahepatic primary tumors such as colon cancer.
- Viable tumor in the treatment zone manifests as contrast enhancement at arterial phase dynamic CT or MR imaging of HCC. Arterial phase imaging is recommended because it provides optimal contrast between viable vascularized HCC and nonenhancing necrotic tissue.
- Directed therapies often affect tumor viability before changes in tumor size can be seen at imaging. Therefore, estimation of necrosis and viable tumor volume is a more sensitive biomarker for assessing success of local-regional therapies.

Imaging is integral to the care of patients undergoing targeted therapy and is used to select patients, guide treatment delivery, and assess treatment effectiveness (2,7,26–29). Pretreatment imaging is essential to define tumor burden and stage, determine the relationship of tumor to critical structures, select appropriate therapeutic options, and plan treatment delivery (2,7,26–29). Postprocedural imaging is required to monitor therapeutic success and detect residual or recurrent disease to guide future therapy (7,26–29). Technical advancements in cross-sectional imaging techniques such as computed tomography (CT) and magnetic resonance (MR) imaging, coupled with innovations in postprocessing capabilities, have not only facilitated reliable morphologic assessment of hepatobiliary tumors but also enabled functional evaluation. Image fusion software allows coregistration of various imaging methods such as CT, ultrasonography (US), MR imaging, and positron emission tomography (PET), which can assist in procedural planning and treatment delivery. Volumetric assessment of tumors and nontumoral hepatic parenchyma is increasingly used to plan therapy and improve assessment of posttreatment response. Molecular imaging techniques such as fluorodeoxyglucose (FDG) PET and hybrid PET/CT offer opportunities to evaluate various physiologic properties of tumors. This review describes the role of imaging in preprocedural evaluation and postprocedural assessment of hepatobiliary malignancies in patients undergoing image-guided targeted therapy.

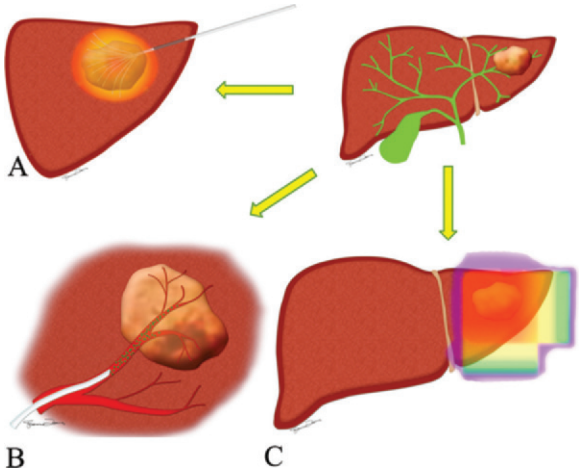

Figure 1. Drawings show local-regional therapies for hepatobiliary malignancy (top right): *A,* percutaneous ablation; *B,* intra-arterial therapy; and C, image-guided radiation treatment (IGRT).

Treatment Principles

Percutaneous Tumor Ablation

Percutaneous image-guided ablative techniques include ethanol injection, RFA, microwave ablation, cryoablation, laser ablation, and irreversible electroporation. The fundamental principle of percutaneous ablation is to achieve local tumor control by inserting chemicals, heat, or electric current into the tumor through a needle or needle electrode to enable in situ destruction of hepatic malignancy while preserving surrounding normal liver parenchyma (30–33). It is a promising substitute for surgery in well-selected patients with HCC and is also increasingly being performed in patients with liver-limited oligometastatic disease from colon cancer, neuroendocrine tumors, or thyroid cancer (6,30–33). Modalities commonly applied in the liver include ethanol injection, RFA, and microwave ablation, while irreversible electroporation, cryoablation, and laser ablation are less commonly performed in the liver because of limited clinical experience (Table 1). Among the various ablative techniques, collective experience with RFA is much higher, and RFA is considered a standard treatment option for local tumor control (7,14,32,34–36).

Intra-arterial Therapies

Intra-arterial therapies such as transarterial embolization, TACE, and SIRT accomplish tissue destruction by transarterial administration of different particles into vessels that supply tumors (13,14). Transarterial embolization techniques are

Table 1: Local-Regional Therapies for Hepatobiliary Malignancies

Therapy	Treatment Criteria by Tumor Type	
	HCC	Metastases
Percutaneous ablation		
Ethanol injection (absolute or 95% alcohol): causes chemically induced coagulative necrosis	Patients who are poor surgical candidates because of inadequate liver function from underlying cirrhosis or prior liver resection or because of significant comorbid conditions (cardiac or respiratory disease); patients ineligible for surgical resection because of the anatomic distribution of liver tumors; bridge to liver transplantation for local tumor control; treatment efficacy comparable to that of RFA for solitary HCCs <3 cm	Most centers treat patients with lesions <5 cm; limited data on role of ethanol ablation in patients with liver metastases
RFA: thermal ablative technique that transmits high-frequency alternating current into tumor to induce coagulation necrosis	Preferred option (6–9); patients who are poor surgical candidates because of inadequate liver function from underlying cirrhosis or prior liver resection or because of significant comorbid conditions (cardiac or respiratory disease); patients ineligible for surgical resection because of the anatomic distribution of liver tumors; bridge to liver transplantation for local tumor control	Most centers treat patients with lesions <5 cm; relative contraindications are lesions adjacent to the liver surface, hepatic hilum (thermal injury to bile duct), or large hepatic vessels (heat sink phenomenon)
Microwave ablation: thermal ablative technique that uses microwaves with frequencies >900 kHz to cause coagulation necrosis	Same patient criteria as for RFA; microwave ablation is preferred for large tumors (≥6 cm) and tumors close to vessels (10)	Most centers treat patients with lesions <5 cm
Irreversible electroporation: nonthermal ablative technique that uses high-voltage (3 kV) electric pulses to cause permanent increase in cell membrane permeability	Same patient criteria as for RFA; limited data on role of irreversible electroporation in treatment of patients with HCC; however, there are advantages compared to thermal ablative techniques for treatment of tumors close to vessels, bile ducts, and critical structures	Most centers treat patients with lesions <5 cm; limited data on role of irreversible electroporation in patients with liver metastases
Intra-arterial therapies		
TACE: injection of intra-arterial embolic material causes exclusive ischemic necrosis of tumor	First-line noncurative or palliative option for nonsurgical patients with large or multifocal HCC without major vascular invasion or extrahepatic disease and preserved performance status and liver function (11–15)	Palliative option for patients with chemorefractory metastatic colorectal cancer, neuroendocrine tumor, or breast cancer (15)
SIRT: Intra-arterial administration of radioisotopes causes brachytherapy-like selective tumor destruction	Patients with good overall functional performance and liver reserve (Child-Pugh class A or B lesions) and tumors confined to the liver that are not amenable to resection or ablation (15)	Combined with systemic chemotherapy in patients with advanced colorectal cancer (15); limited data in patients with liver metastases from neuroendocrine tumors and breast cancer (15)

Note.—HCC = hepatocellular carcinoma, RFA = radiofrequency ablation, SIRT = selective internal radiation therapy, TACE = transarterial chemoembolization.

(continues)

Table 1: Local-Regional Therapies for Hepatobiliary Malignancies *(continued)*

Therapy	Treatment Criteria by Tumor Type: HCC	Treatment Criteria by Tumor Type: Metastases
IGRT		
Targeted tumor destruction through focused high-energy radiation or proton beam that causes DNA damage and cell death	Unresectable locally advanced HCC (nodular, diffuse, large with intrahepatic metastases or tumor invasion of the hepatic or portal vein) without extrahepatic metastases (16–18); Child-Pugh class A or B lesions; tumors occupying less than two-thirds of the liver (16–18); recurrent or refractory HCC after nonsurgical treatment (RFA or TACE) (16–18); HCC with malignant portal vein thrombosis (16–18)	Patients with metastases not amenable to other local therapies (19,20), one to five metastases (19,20), limited tumor size (<6 cm) (19,20), locally controlled primary site, favorable histology (breast or colorectal cancer), young age and good performance status, at least 700 mL of uninvolved liver volume, and adequate pretreatment baseline liver function

Note.—HCC = hepatocellular carcinoma, RFA = radiofrequency ablation, SIRT = selective internal radiation therapy, TACE = transarterial chemoembolization.

feasible because of the dual hepatic vascular supply from the portal vein (75%) and hepatic artery (25%) (13,14). Because blood supply to a hepatic tumor is preferentially arterial, intra-arterially administered embolic agents and chemotherapeutic drugs distribute selectively within tumors, initiating acute obstruction of feeding arteries with subsequent exclusive ischemic necrosis (13,14). Since the tumor-free normal liver is supplied by the portal vein, intra-arterial therapies limit damage to the rest of the liver parenchyma (13,14). While transarterial embolization involves selective instillation of embolic materials (eg, Gelfoam [Pharmacia & Upjohn], polyvinyl alcohol) into the hepatic arteries, TACE refers to administration of chemotherapeutic agents (doxorubicin, cisplatin, or mitomycin C) with or without ethiodized oil in combination with embolic particles to increase the efficacy of tumor destruction (13,14). SIRT, or radioembolization, is a form of brachytherapy that involves intra-arterial administration of micron-sized particles (20–60 μm) containing yttrium 90 (^{90}Y), which deliver focused β radiation to cause tumor destruction while minimizing radiation damage to the surrounding normal liver (13–15). Unlike TACE, SIRT requires preservation of adequate perfusion to the tumor to enhance free radical–dependent cell death from radiation therapy (13–15). In addition to their role in treating locally advanced disease, intra-arterial therapies are increasingly used as an adjunct to RFA to downstage tumors before surgical resection and as a bridge to liver transplantation (Table 1) (13,14).

Image-guided Radiation Therapy

External beam radiation therapy has conventionally been unsuccessful in treatment of hepatobiliary malignancies because the radiation dose necessary for treatment of HCC (70–90 Gy) exceeds the tolerance limits of the liver (25). External beam radiation doses greater than 35 Gy often result in radiation-induced liver disease (25). With the introduction of three-dimensional conformal radiation therapy, there has been rising interest in use of targeted radiation therapy, which allows focused delivery of a high radiation dose to a small volume of the liver while limiting irradiation of residual functional liver parenchyma and surrounding structures (20). IGRT uses a stereotactic approach with orthogonal radiographs to help visualize percutaneously placed radiopaque fiducial markers around the tumor and permits high-precision radiation delivery (23). Use of a focused high-energy radiation beam (x-rays or gamma rays) or proton beam leads to DNA damage, which causes cell death and destruction of the targeted tumor (Fig 1). Advances in image-guided radiation delivery techniques and improved strategies to counter patient motion have allowed superior local tumor control and limited peripheral toxic effects (20,25). IGRT is increasingly being used to treat hepatobiliary malignancies, particularly liver metastases that are not suitable for surgical or ablative therapy (20,25).

Treatment Planning

General Considerations

Imaging plays a central role in initial evaluation of patients diagnosed with malignant hepatobiliary tumors and is crucial in selecting the most appropriate local or systemic treatment (eg, surgical resection vs systemic chemotherapy or

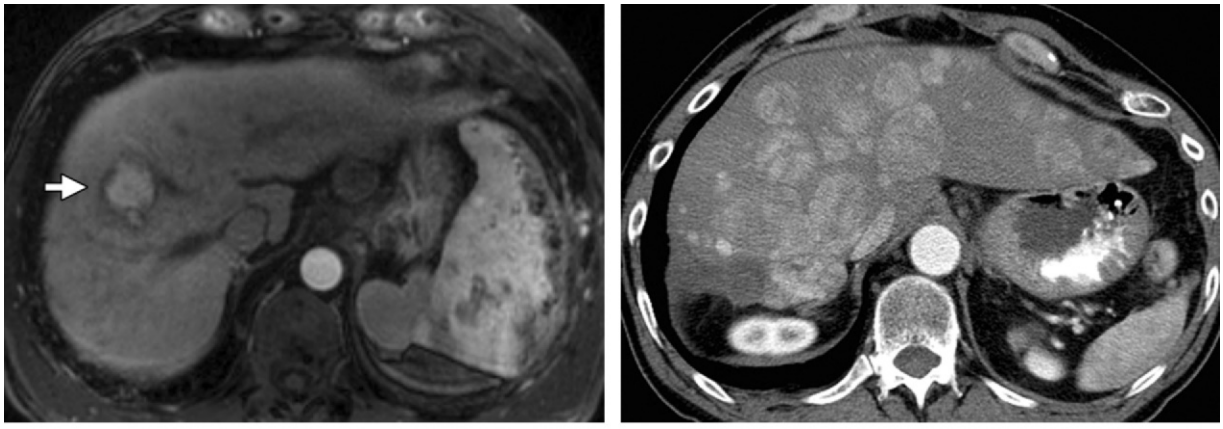

a. b.

Figure 2. Tumor staging for selection of local-regional treatment. **(a)** Axial gadolinium-enhanced MR image in a 60-year-old man shows a 2.9-cm arterially enhancing HCC (arrow), which was later treated with RFA. **(b)** Axial contrast-enhanced CT image in a 77-year-old man shows multiple arterially enhancing lesions in both lobes of the liver, findings that were demonstrated at biopsy to be HCC and were treated with TACE.

local-regional therapy). Patient selection often requires a multidisciplinary collaborative effort and is based on oncologic assessment as well as technical feasibility of various treatment options (37). Imaging is indispensable because it often obviates needle biopsy by allowing accurate diagnosis and characterization of hepatic tumors (eg, HCCs) (2). In fact, optimal imaging evaluation before treatment initiation has been shown to change management strategies in nearly 30% of patients with liver metastases from colorectal cancer who were treated at tertiary care centers (28).

The imaging protocol for staging of hepatic malignancies should be tailored to the individual tumor type (7). In patients with HCC or liver metastases, dynamic multiphasic contrast-enhanced CT and dynamic gadolinium-enhanced MR imaging (including arterial, portal venous. and delayed phases) are accepted options for initial diagnostic evaluation, regardless of the type of therapy that will be selected (1,7). Success of ablative techniques is influenced by accurate definition of hepatic tumor burden and tumor relationship to surrounding critical structures and vessels; for this reason, MR imaging may be preferred because of its superior contrast resolution (37). In patients with liver metastases rather than HCC, hepatocyte-specific contrast agents such as gadoxetate disodium increase accuracy for lesion detection and characterization, particularly in tumors smaller than 10 mm (38–41). Several studies have shown that irrespective of tumor size, detection of liver metastases is significantly improved on delayed hepatobiliary phase images owing to superior liver-lesion definition created by hypointense metastases and avid uptake of gadolinium contrast agent by background normal liver (39–42). Gadoxetate disodium–enhanced MR imaging has been reported to have high sensitivity (95%) and specificity (94%) for detection of liver lesions and reportedly results in a change in planned surgical therapy in 14.5% of patients (43–45). In our experience, radiation oncologists prefer gadoxetate disodium–enhanced hepatobiliary phase MR imaging to facilitate more restricted delivery of therapies such as proton beam or x-ray radiation. In high-risk patients with cancers other than HCC, fluorine 18 FDG PET or PET/CT may also be necessary to exclude extrahepatic metastatic disease (7). In patients with liver-limited metastases detected at imaging, chest CT is often performed additionally to rule out extrahepatic disease (7).

Tumor Staging and Factors in Treatment Selection

Tumor Size and Number.—The principal role of pretreatment imaging is to help determine tumor burden and accurately stage hepatic malignancy by evaluating tumor size, number, and location; vascular involvement; nodal spread; and extrahepatic metastases to allow selection of the most appropriate targeted therapeutic option (7,37). Tumor burden (ie, size and number of hepatic tumors) forms an important basis for selection of the appropriate local-regional therapy (7,28,29,46). Simplistically stated, patients with a solitary tumor or up to three tumors are often treated with percutaneous ablation or IGRT, while patients with multiple hepatic lesions are better treated with intra-arterial therapies (Fig 2) (7). When percutaneous ablation is selected, tumor size has considerable influence on the treatment plan, including determination of type and number of electrode probes (eg, single

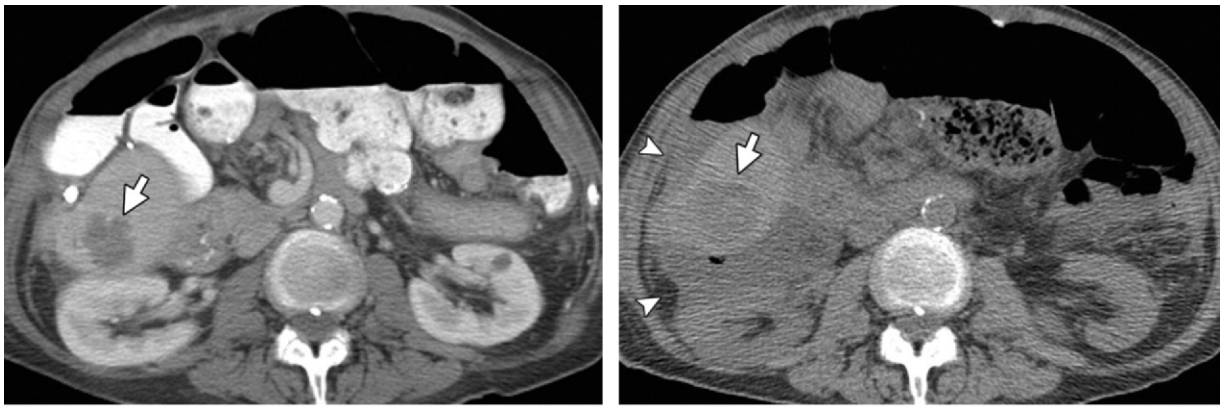

a. b.

Figure 3. Effect of tumor location on planning for percutaneous ablation. **(a)** Axial contrast-enhanced CT image shows a solitary metastasis from colorectal cancer in the inferior segment of the liver (arrow), close to the kidney and colon. **(b)** Axial intraprocedural CT image shows 5% dextrose solution instilled intraperitoneally (arrowheads) to move the colon and kidney away from the lesion (arrow) and facilitate successful RFA.

vs clustered probes) (28,37,46,47). Tumor size is a strong predictor of treatment success and survival in patients with primary or metastatic liver malignancies, as demonstrated in several studies (7,28,29,46). In patients diagnosed with early-stage HCC with preserved liver function (Child-Pugh score of A or B) and/or those with limited tumor burden (ie, a solitary HCC <5 cm or three or fewer nodular HCCs <3 cm), percutaneous ablation is preferred for nonsurgical candidates (7). In patients with HCC, effectiveness of the ablative procedure has a direct correlation with tumor size, with smaller tumors (≤5 cm) demonstrating a higher likelihood of favorable outcome (46). In particular, patients with tumors smaller than 3 cm treated with ablation have outcomes matching those of patients with surgically resected tumors (46). Patients with HCCs larger than 5 cm are generally not considered ideal candidates for percutaneous ablation, and surgical resection remains a favored option (29). Multifocal HCC with several liver lesions of varying sizes indicates a possibility of intrahepatic metastases and advanced disease; these patients have poor outcomes and are not suitable candidates for resection (29). In patients with cirrhosis and multifocal HCC who meet transplant criteria, liver transplantation is the best treatment option (29).

There is less consensus on optimal guidelines for use of local-regional therapies in patients with hepatic metastases from extrahepatic primary malignancies (28). Surgical resection is the preferred curative treatment for liver-only metastases from colorectal cancer, but ablative therapies and IGRT are increasingly being offered as alternatives in patients who decline surgery or when surgery is contraindicated because of medical comorbidities (26). In nonsurgical candidates with liver-confined oligometastatic disease (fewer than five liver lesions), RFA has shown some success in controlling tumor burden, with a 5-year survival rate of 24%–44% in patients with tumors smaller than 5 cm (7,19,26,32,48,49). At most experienced centers, thermal ablation is used in patients with solitary tumors or five or fewer tumors measuring 3 cm or less (6,7,28,49). There is considerable evidence that patients with colorectal liver metastases smaller than 3 cm have favorable outcomes, with a reported 5-year survival rate of 55%–56% , compared with patients with tumors larger than 3 cm (30%–42% survival rate) (6,21). Tumor recurrence rates after RFA in patients with metastatic colorectal cancer vary from 6% to 40% and are relative to lesion size, number, and location, with worsening outcomes for patients with tumors larger than 5 cm (7,28,49). Higher rates of complete ablation can be achieved with microwave ablation because of the larger ablation zone (7). In patients for whom ablation is not feasible or not an option, intra-arterial methods such as TACE (with irinotecan administration) and SIRT are promising but less-established approaches (7). For patients with hepatic metastases from other primary cancers (eg, melanoma or thyroid cancer), there are limited data on the effect of tumor size and number on selection of local-regional therapies, but these therapies could be used for local tumor control (6,7).

Tumor Location.—Tumor location has major implications for planning ablative, intra-arterial, and radiation therapies because it not only dictates the type of local-regional therapy but also the percutaneous approach to the tumor. In patients undergoing percutaneous ablation, precise delineation of tumor location helps determine the needle trajectory or path to the tumor and type of ablative technique selected (eg, RFA vs

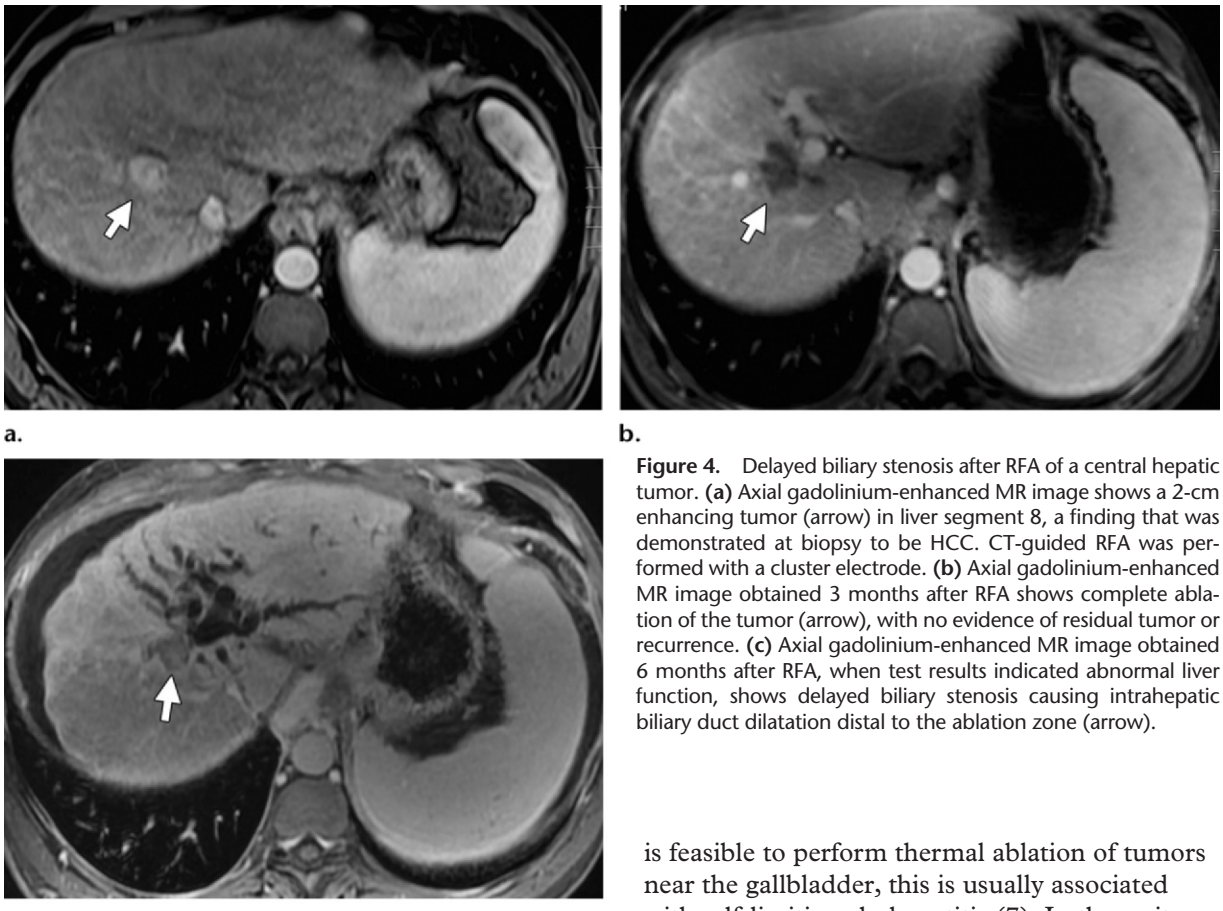

Figure 4. Delayed biliary stenosis after RFA of a central hepatic tumor. **(a)** Axial gadolinium-enhanced MR image shows a 2-cm enhancing tumor (arrow) in liver segment 8, a finding that was demonstrated at biopsy to be HCC. CT-guided RFA was performed with a cluster electrode. **(b)** Axial gadolinium-enhanced MR image obtained 3 months after RFA shows complete ablation of the tumor (arrow), with no evidence of residual tumor or recurrence. **(c)** Axial gadolinium-enhanced MR image obtained 6 months after RFA, when test results indicated abnormal liver function, shows delayed biliary stenosis causing intrahepatic biliary duct dilatation distal to the ablation zone (arrow).

microwave ablation) and also influences other aspects of percutaneous treatment, such as patient positioning, type of electrode used, and need for adjunctive procedures (eg, hydrodissection) (37). Careful definition of the anatomic location of the tumor in the liver and its relationship to surrounding structures such as the stomach, colon, and gallbladder is critical during pretreatment image review because these factors can affect treatment efficacy and increase the complication rate (7,37,47). For example, thermal ablation of superficial tumors located near the liver surface close to parts of the gastrointestinal tract can lead to thermal injury and perforation of the gastric or bowel wall (7). Several authors describe use of adjunctive procedures before thermal ablation, including hydrodissection or intraperitoneal instillation of dextrose fluid into the space between the liver and adjoining bowel loops to displace these structures from the tumor and limit injury to hollow organs (Fig 3) (7,49,50). Intraperitoneal instillation of fluid is also performed before RFA of surface lesions to limit pain from peritoneal irritation caused by ablation (7,50). Hydrodissection performed before percutaneous ablation of hepatic dome lesions restricts diaphragmatic injury (7,50). Although it is feasible to perform thermal ablation of tumors near the gallbladder, this is usually associated with self-limiting cholecystitis (7). In these situations, use of nonthermal ablative techniques such as percutaneous ethanol injection or irreversible electroporation could be considered.

Percutaneous thermal ablation of tumors near the liver hilum increases risk for biliary injury, particularly to the common hepatic duct (7,37,49,51). Delayed biliary stenosis has been reported, particularly for tumors located less than 1 cm from large biliary ducts (Fig 4) (7,37,49,51). Careful delineation of the tumor's relationship to large vessels is also important. Percutaneous ablation of tumors near hepatic vessels is feasible, and thermal injury to vessel walls is limited because of flowing blood. However, proximity to these vessels can limit the efficacy of RFA because of possible heat sink (49). Reports have suggested local recurrence rates of nearly 48% for tumors situated close to large vessels owing to inadequate treatment of tumor tissue close to the vessel due to loss of heat by convection (6,7,49). Some authors have suggested temporary percutaneous balloon occlusion of large hepatic or portal veins during RFA of tumors larger than 3 cm that are close to hepatic and portal vein branches larger than 4 mm (52). A reported advantage of microwave ablation is lower susceptibility to heat sink; in certain situations, microwave ablation is preferable to RFA for tumors close to large vessels (14,33).

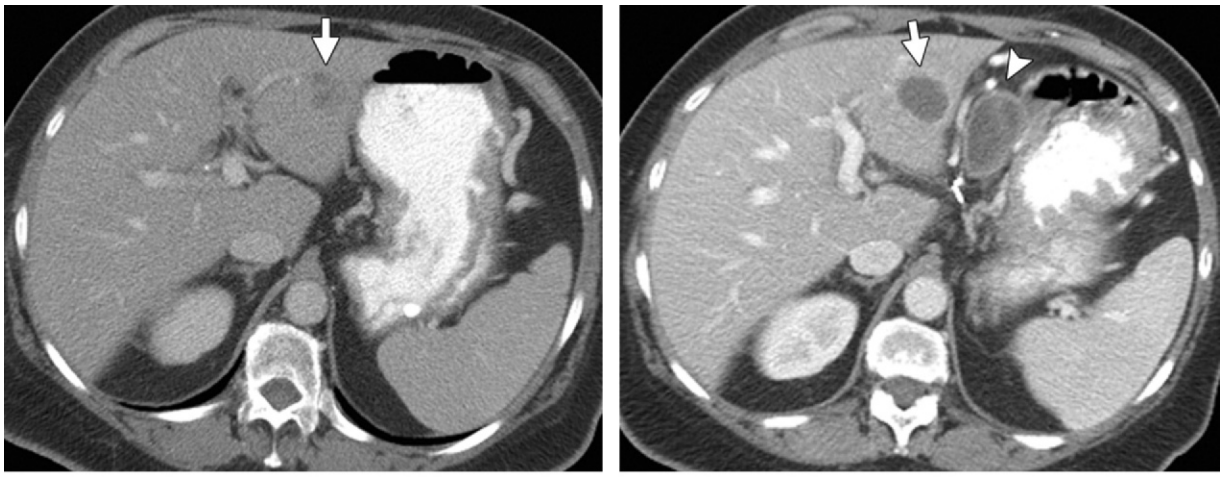

a. b.

Figure 5. Effect of tumor location on planning for IGRT. **(a)** Axial contrast-enhanced CT image shows a hypoattenuating metastasis from colon cancer in the lateral segment of the left lobe of the liver (arrow). Its proximity to the stomach increases risk for radiation injury to the stomach, and a biologic mesh spacer (not shown) was surgically placed between the liver and stomach to facilitate IGRT. **(b)** Axial contrast-enhanced posttreatment CT image shows the treated tumor (arrow) and biologic mesh spacer (arrowhead).

a. b.

Figure 6. Pretreatment imaging to assess vascular involvement in a 62-year-old man before local-regional therapy. **(a)** Axial contrast-enhanced CT image shows a large right cholangiocarcinoma (arrow) invading the right portal vein. **(b)** Axial maximum intensity projection CT image better depicts portal vein (*PV*) invasion by the tumor (arrows).

For intra-arterial therapies such as TACE and SIRT, determination of tumor location in the liver is essential at CT or MR imaging to allow selection of the target hepatic artery for cannulation before embolization (see the section on "Vascular Anatomy"). In patients undergoing targeted radiation therapy, assessment of tumor location is crucial to avoid radiation injury to adjacent normal structures in or surrounding the liver (eg, breast, stomach, and small and large bowel). In fact, surgical placement of biologic mesh spacers (Alloderm; Lifecell, Branchburg, NJ) is being performed before radiation therapy to move adjacent structures from the radiation field and minimize damage (Fig 5) (53,54).

Local Tumor Invasion and Extrahepatic Disease.—Tumor invasion into the portal and hepatic veins adversely affects patient outcome and overall survival and is a relative contraindication to local-regional therapies (29,37). Risk for vascular invasion increases with increasing tumor size, and surgical resection of these tumors is debatable (29). Multiplanar reformations, particularly with coronal and sagittal views and maximum intensity projections, are particularly helpful for delineating vascular invasion. The presence of venous thrombosis (tumor or bland thrombus) is also important because substantial venous occlusion in the setting of borderline hepatic function precludes use of local-regional therapies such as TACE or SIRT (Fig 6) (47). Tumor thrombosis or invasion of the main portal trunk, main hepatic vein, or larger branches is associated with a poorer prognosis than is involvement of second-order branches of the

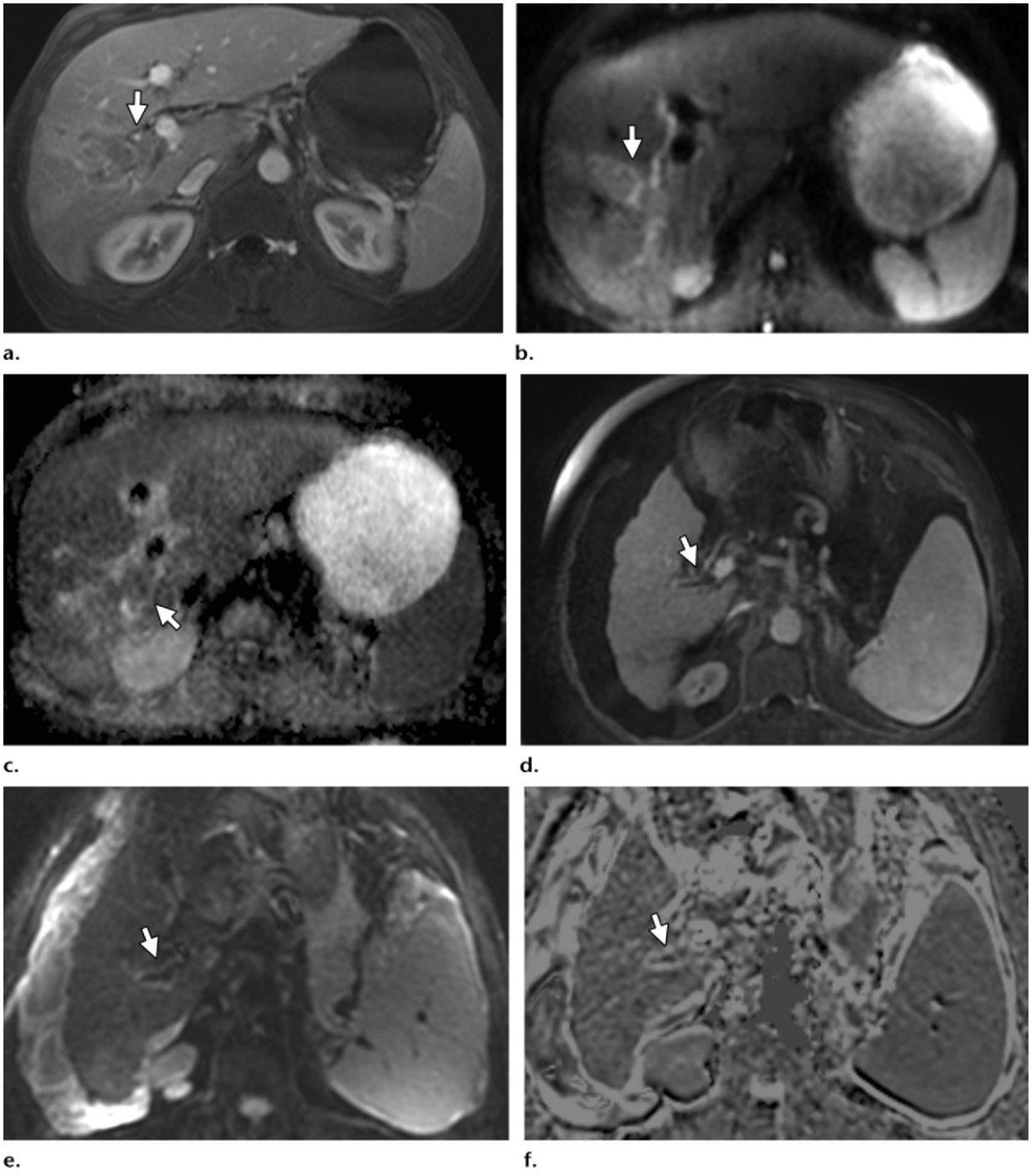

Figure 7. Diffusion-weighted imaging for evaluation of venous thrombosis. **(a–c)** In a 63-year-old man, axial gadolinium-enhanced MR image **(a)** shows an infiltrative HCC with tumor thrombus (arrow) in the portal vein. Axial diffusion-weighted MR image (b = 600 sec/mm^2) **(b)** shows hyperintensity of the thrombus. Corresponding ADC map **(c)** shows hypointensity of the thrombus, a finding suggestive of restricted diffusion. **(d–f)** In a 55-year-old man with nodular HCC, axial gadolinium-enhanced MR image **(d)** shows a nonocclusive portal vein thrombus (arrow). Axial diffusion-weighted MR image (b = 500 sec/mm^2) **(e)** shows hypointensity of the thrombus. Corresponding ADC map **(f)** shows isointensity of the thrombus, a finding suggestive of no restricted diffusion. The presence of main portal vein thrombosis precludes ablative and intra-arterial therapies.

portal or hepatic vein (29). Diffusion-weighted MR imaging has a potential application in characterization of venous thrombus by enabling differentiation of bland from tumor thrombus. The mean apparent diffusion coefficient (ADC) of tumor thrombus is reportedly significantly lower than that of bland thrombus (Fig 7) (55).

Infiltrative nonencapsulated tumors are less amenable to successful treatment with percutaneous ablation, in contrast to tumors with a well-defined tumor capsule (46). Biliary involvement with evidence of intrahepatic biliary duct dilatation is an important consideration before ablation or intra-arterial therapy because it increases risk for

infectious complications and biliary necrosis and necessitates corrective action before local-regional therapies. Intrahepatic biliary duct dilatation is a relative contraindication to percutaneous ablation.

Because percutaneous ablation and radiation therapies are intended for local tumor control, the presence of extrahepatic metastases should be excluded before treatment initiation because they adversely affect outcome and preclude use of local-regional therapies (37). In certain circumstances, percutaneous management of liver metastases from colorectal cancer is feasible in patients with limited extrahepatic disease that can be sufficiently treated (eg, limited bone or pulmonary metastases) (7,37). Patients with advanced HCC and evidence of vascular invasion and extrahepatic disease benefit from systemic chemotherapy or, more recently, ^{90}Y SIRT (7).

Vascular Anatomy.—Preprocedural evaluation of vascular anatomy, particularly arterial anatomy, is valuable in patients undergoing intra-arterial therapies such as TACE or SIRT. Careful assessment of hepatic arterial anatomy, its variants, any hepatofugal flow, and any coexisting vascular diseases (including degree of arterial atherosclerosis) is essential when planning intra-arterial therapies (47). Extrahepatic collateral arteries that supply the liver (eg, accessory hepatic arteries from superior mesenteric, renal, or internal mammary arteries) require particular attention to ensure effective tumor embolization (47). In addition, mapping of arterial anatomy before SIRT facilitates prophylactic embolization of vessels such as the gastroduodenal and right gastric arteries to avoid nontarget embolization of radioactive microspheres into vessels supplying the stomach and small bowel, which can cause intractable radiation ulcers. For the same reason, selective injection of macroaggregated albumin particles into the hepatic artery, followed by single photon emission computed tomography (SPECT), is performed to detect arteriovenous shunting into gastrointestinal or pulmonary vasculature. Collateral vessels with hepatopetal flow and substantial arteriovenous fistulas should be recognized and embolized before definitive therapy to enhance treatment tolerance and efficacy. The presence of severe lung shunting that is not amenable to resolution by embolization is a contraindication to SIRT.

Tumor Metabolism.—Evaluation of tumor metabolism at PET/CT before local-regional therapy is particularly beneficial in tumors that demonstrate FDG uptake and facilitates assessment of treatment response. In patients with hepatic metastases, PET/CT allows detection of extrahepatic disease, which precludes several local-regional therapeutic options. FDG uptake is variable in HCCs and occurs in approximately 60% of tumors, with higher uptake seen in biologically more aggressive and higher-grade tumors. This limits the utility of PET/CT in evaluation of HCC (56). However, in patients with liver metastases from colorectal cancer, PET/CT has been reported to be superior to CT alone for detection of extrahepatic disease and more accurate for assessing treatment response and detecting local recurrence after RFA and SIRT (56). PET/CT also improves disease staging and enables treatment selection in patients with thyroid, melanoma, or carcinoid tumors. However, PET/CT has a limited role in evaluation of small liver lesions, particularly liver metastases from colorectal cancer, and pancreatic cancers smaller than 1 cm (57). Dynamic contrast-enhanced MR imaging, with extracellular contrast agents or gadoxetate disodium, is superior to PET/CT for detection of subcentimeter hepatic lesions.

Estimation of Functional Reserve.—The role of imaging in determination of hepatic functional reserve is often underestimated, despite its value in triage of patients with hepatobiliary malignancies to surgery or local ablative therapy (47). Imaging features that indicate liver dysfunction must be paid particular attention and should always be noted in radiology reports (47). Patients with inadequate hepatic functional reserve can develop metabolic failure after liver resection, and local-regional ablative therapies are the preferred first-line treatment option in patients with parenchymal liver disease such as severe fibrosis or cirrhosis (47). US, CT, and MR imaging allow recognition and characterization of hepatic steatosis and cirrhosis, which point toward chronic parenchymal liver disease. Imaging indicators of a higher degree of liver dysfunction include ascites or hydrothorax and markers of substantial portal hypertension, such as splenomegaly and esophageal or gastric varices (47). These findings not only preclude surgery but also necessitate additional pretreatment procedures such as ascitic tap, endoscopy, and variceal ligation (47). Adequate liver reserve is also essential for SIRT because certain portions of normal hepatic parenchyma are damaged by radiation therapy. Background hepatic parenchymal changes can affect the success of percutaneous ablative therapies. For example, percutaneously injected ethanol easily and selectively diffuses within a soft nodular HCC surrounded by a firm cirrhotic liver and causes a higher degree of necrosis. Similarly, thermal ablation of HCCs is more likely to be successful in the setting of background cirrhosis because of the insulating effect of the fibrotic

liver ("oven" effect), which leads to achievement of higher temperatures in the tumor and longer duration of cytotoxic temperatures (46).

Posttreatment Imaging Evaluation

General Considerations

The main objectives of imaging surveillance after local-regional treatment of hepatobiliary malignancies are to define expected normal changes at the treatment site, identify abnormal changes such as residual disease or tumor recurrence, and depict treatment-related complications to allow prompt intervention and guide further management (7,8). Dedicated imaging surveillance is important to evaluate treatment efficacy, predict patient outcome, and detect new areas of disease distant from the treatment site, including extrahepatic disease. Imaging surveillance is particularly useful in patients with metastases to the liver, as they often have a high rate of recurrence not only at the treatment site but also remotely because of development of new extrahepatic metastases (26). The recurrence rate could be as high as 40%–45% for intrahepatic as well as extrahepatic locations (26).

Imaging Protocol

Dynamic multiphasic contrast-enhanced CT and gadolinium-enhanced MR imaging are the standard of care for assessment after image-guided targeted therapies (8,58,59). Gadolinium-enhanced MR imaging is preferred over CT because of its higher specificity and soft-tissue contrast. Subtraction imaging adds value as a complementary technique for precise determination of enhancement in the treatment zone. FDG PET/CT is superior to CT for detection of intra- and extrahepatic recurrences after local-regional therapies, particularly in hepatic metastases from extrahepatic primary tumors such as colon cancer (Fig 8) (56). In patients with liver metastases from colorectal cancer, PET/CT is preferred to CT for evaluation of the ablation zone. Regardless of the technology used, it is imperative to maintain consistency in the imaging protocol used before treatment and at different times after therapy for accurate assessment of response. Imaging assessment is generally performed 4–8 weeks after treatment (7). After this assessment, subsequent follow-up imaging is performed to detect local tumor progression (evidenced by recurrence and new hepatic or extrahepatic sites of disease) (7). Our current institutional practice includes follow-up imaging at 1, 3, 6, 9, and 12 months after treatment, followed by imaging at longer intervals as appropriate for the underlying disease if no residual or recurrent disease is seen.

Imaging Appearances

Percutaneous Ablation.—Expected changes at the ablation site vary according to time elapsed after the procedure and evolve over time (7,8). Regardless of the type of ablative technique used, a surrounding circumferential rim of normal liver tissue, usually 1-cm thick, is ablated with the viable tumor to obtain a tumor-free margin and ensure effective eradication of microscopic invasion around the tumor periphery while preserving normal hepatic function. As a result, the final ablation zone is usually larger than the tumor dimensions (Table 2) (Figs 9, 10) (7,8). In immediate postablation CT images, it is not uncommon to see small air bubbles in the ablation zone or portal vein, which usually are caused by tissue necrosis (47). After intravenous contrast agent administration at CT or MR imaging, completely ablated tumor typically demonstrates total lack of enhancement in the arterial, portal venous, and delayed phases, which indicates successful treatment. A thin rim of peripheral enhancement around the ablation zone represents a benign inflammatory reaction to thermal injury with formation of granulation tissue and has a relatively concentric, symmetric, uniform appearance with smooth inner margins. This finding should be differentiated from irregular nodular enhancement of residual tumor seen at the periphery of the ablation zone (7,8). In addition, wedge-shaped peripheral areas of arterial enhancement in the hepatic parenchyma adjacent to the ablated area, which are related to areas of arteriovenous shunting from needle puncture or thermal injury, can be seen (7). When areas of enhancement are not discernible from recurrent tumor, close interval follow-up imaging should be performed. Areas of recurrence will show interval growth, while perfusional variants disappear or become smaller at follow-up imaging (7). Eventually, the ablation zone becomes homogeneously hypoattenuating, with reduction in size secondary to fibrous tissue and nonenhancing scar formation (47). Dystrophic calcification and capsular retraction in peripheral lesions have also been described (47).

Abnormal imaging appearances include immediate or delayed atypical changes that suggest inadequate treatment, disease progression, or complications (7). Incomplete ablation with residual tumor is seen as nodular enhancing areas in the treatment zone (Fig 11). Intrahepatic recurrence after local-regional therapy could represent local tumor progression at the margin of the treatment zone or distant recurrence due to new tumor away from the ablation zone (60). Careful posttreatment evaluation of the liver is imperative because new tumors could arise remote from the initial ablation

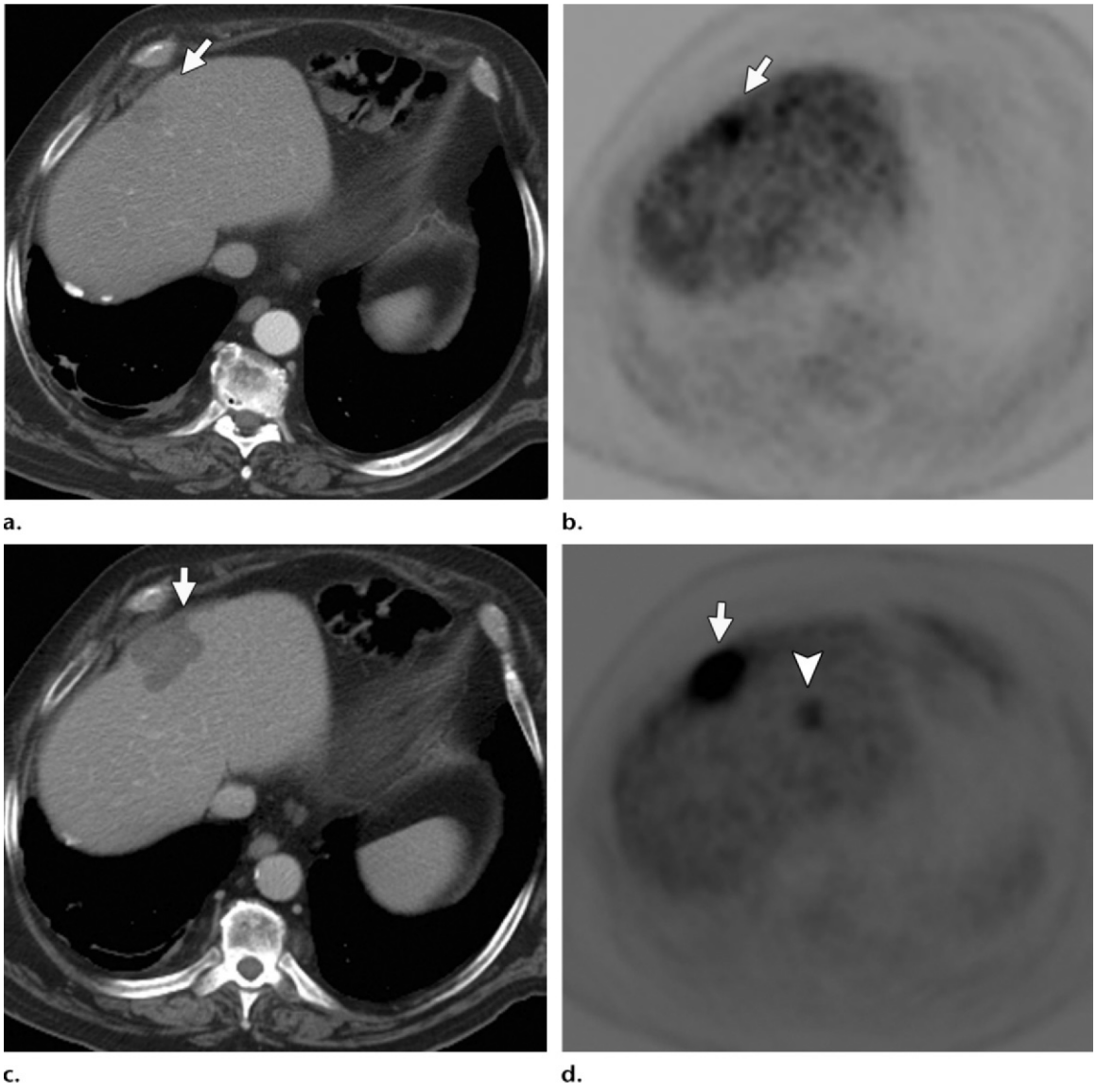

Figure 8. Imaging evaluation after percutaneous ablation of a liver metastasis from rectal cancer in a 55-year-old man. **(a)** Axial contrast-enhanced pretreatment CT image shows a subtle, 1.5-cm, hypoattenuating lesion (arrow) in the dome of the liver. **(b)** Corresponding axial PET image shows intense FDG avidity in the lesion (arrow). The metastatic deposit was treated with RFA. **(c)** Axial contrast-enhanced CT image obtained 3 months after RFA shows the ablation zone (arrow) with no features of recurrent disease. **(d)** Corresponding PET image shows intense FDG avidity in the ablation zone (arrow), a finding indicative of tumor progression, and a new FDG-avid metastatic deposit (arrowhead) not seen at CT.

site because of growth of micrometastases or new metastases (26). Tumor recurrence in the ablation zone appears as new areas of nodular enhancement after previous imaging confirmation of complete ablation. The pattern of residual tumor or local recurrence is generally similar in primary hepatic tumors and hepatic metastases. However, in liver metastases from colorectal cancer, tumor recurrence is difficult to discern at arterial phase imaging because of the hypovascular nature of the tumor (26). Nodular pattern, halo pattern, and gross enlargement have been described as various manifestations of recurrent liver metastases from colorectal cancer that are better visualized in the portal venous phase (26). The halo pattern is seen as a thick rim of viable tumor and should not be confused with the thin rim of benign peripheral enhancement (26). PET/CT performed shortly after RFA provides crucial information on the success of tumor ablation by allowing differentiation of posttreatment changes from residual or recurrent malignant tumor, thereby aiding in early reintervention (Fig 8) (56). However, PET/CT may not be ideal for detection of small nodular recurrences (<1 cm), and false-positive findings can occur in rare occasions of infective complications and abscess formation at the treatment site (56).

Intra-arterial Therapies.—Imaging findings after TACE often depend on the type of embolic

Table 2: Imaging Appearances after Local-Regional Therapies

Type of Therapy	Appearance at CT	Appearance at MR Imaging
Percutaneous ablation	Nonenhanced: hypoattenuating or heterogeneously hyperattenuating; areas of hyperattenuation correspond to areas of hemorrhage or proteinaceous material Contrast-enhanced: ablation zone appears as nonenhancing area with larger diameter than original tumor; central nonenhancing area (necrotic tissue) with thin uniform rim of peripheral enhancement (granulation tissue); additional features include area of arterial phase enhancement in surrounding hepatic parenchyma	Nonenhanced: heterogeneously hyperintense on T1-weighted images and hypointense on T2-weighted images; areas of T1 hyperintensity correspond to areas of hemorrhage or proteinaceous material; T2 hypointensity is predominantly due to dehydration and coagulation necrosis Contrast-enhanced: ablation zone appears as nonenhancing area with larger diameter than original tumor; central nonenhancing area (necrotic tissue) with thin uniform rim of peripheral enhancement (granulation tissue); additional features include area of arterial phase enhancement in surrounding hepatic parenchyma
Intra-arterial therapies	Nonenhanced: variably hypoattenuating; after TACE with iodized oil, hyperattenuation in the lesions corresponds to iodized oil uptake Contrast-enhanced: complete necrosis is seen as absence of enhancement on arterial and portal venous phase images	Nonenhanced: hyperintense areas on T1-weighted images and hypointense areas on T2-weighted images Contrast-enhanced: lack of tumor enhancement on gadolinium-enhanced images, with thin peripherally enhancing pseudocapsule in arterial phase
IGRT	Nonenhanced: mild well-demarcated area of hypoattenuation corresponding to radiation zone Contrast-enhanced: tumor tissue does not enhance; irradiated region demonstrates more intense enhancement than surrounding liver tissue; contrast enhancement is sustained longer in delayed phase; zone of radiation is well demarcated from the rest of liver parenchyma	Nonenhanced: hypointense on T1-weighted images and slightly hyperintense on T2-weighted images Contrast-enhanced: tumor tissue does not enhance; irradiated region shows more intense enhancement than surrounding liver tissue; contrast enhancement is sustained longer in delayed phase; radiation zone is well demarcated from rest of liver parenchyma

agent administered. After TACE performed with iodized oil, therapeutic response is evaluated according to deposition of iodized oil in tumors at nonenhanced CT and tumor size and enhancement at contrast-enhanced CT or gadolinium-enhanced MR imaging (7). Nonenhanced CT images demonstrate tumor uptake of iodized oil as hyperattenuating areas, and the degree of iodized oil uptake is proportional to the degree of tumor necrosis (7) (Fig 12). Although uptake of iodized oil at nonenhanced CT is a useful marker of tumor necrosis, the presence of iodized oil limits assessment of enhancement on contrast-enhanced CT images and often results in underestimation of residual viable tumor (7). However, the signal characteristics of treated tumor at MR imaging are not affected by deposition of iodized oil, and gadolinium-enhanced MR imaging is therefore more useful than CT to depict abnormal enhancement (Fig 13) (7). Treated HCC can have variable signal intensity on T1- and T2-weighted MR images (Table 2) (47). In general, necrotic tumors are hypointense on T2-weighted images, with hyperintense foci likely representing hemorrhage or residual tumor (47). Dynamic multiphasic contrast-enhanced CT and gadolinium-enhanced MR imaging are useful in patients who undergo conventional TACE or transarterial embolization without iodized oil administration; in such cases, CT is as effective as MR imaging for monitoring treatment response (Fig 14) (7).

After SIRT, response assessment is performed by estimating the reduction in tumor enhancement (7). The ^{90}Y administered during SIRT has a half-life of 2.67 days; as a result, over 90% of the radiation is delivered in 11 days (7). In patients with HCC, there is complete lack of enhancement in the arterial and portal venous phases of gadolinium-enhanced MR imaging

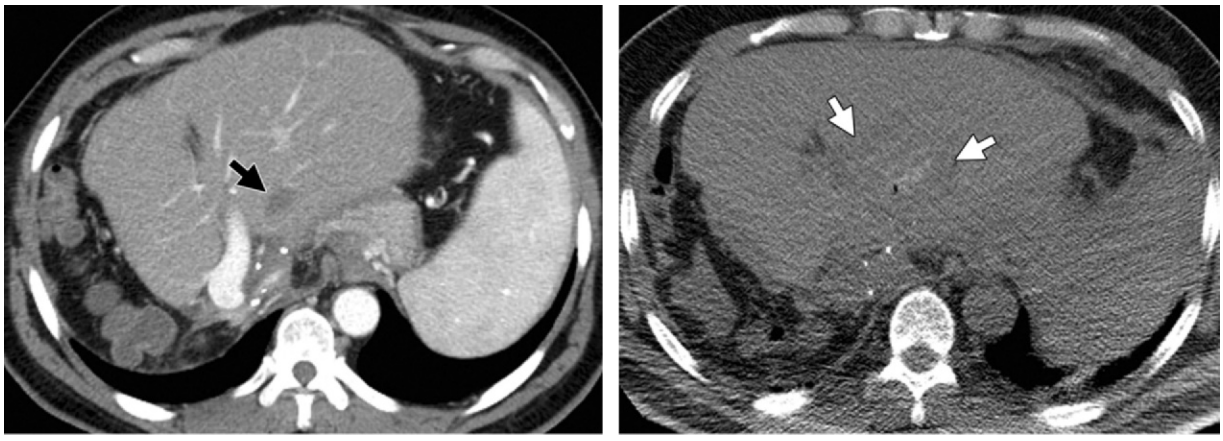

Figure 9. Expected changes seen at CT after RFA of a liver metastasis from colorectal cancer. **(a)** Axial contrast-enhanced pretreatment CT image shows a 2-cm metastatic lesion in the left hepatic lobe (arrow). **(b)** Axial nonenhanced CT image obtained 1 month after RFA shows hyperattenuation in the ablation zone (arrows), a finding likely corresponding to hemorrhage, necrosis, and debris. **(c)** Axial contrast-enhanced CT image obtained 1 month after RFA shows that the nonenhancing ablation zone (arrows) is larger than the metastatic lesion seen in **a**, a finding indicative of complete treatment response.

after successful treatment (Fig 15) (7). Substantial changes in tumor size may not be seen in the initial few months after treatment (7). A transient peripheral rim of enhancement may be seen around the tumor and is due to local radiation effects, which may last for several months (7). Transient inflammatory changes may be seen within the liver and should not be confused with tumor progression (7). These manifestations include areas of periportal hypoattenuation due to perivascular edema, hypertrophy of the contralateral lobe and atrophy of the ipsilateral lobe, perihepatic ascites resulting from the effects of radiation on the Glisson capsule, and sympathetic pleural effusion (7). In patients with liver metastases from colorectal cancer who undergo SIRT, PET/CT has been shown to be useful for accurate assessment and quantification of metabolic response after treatment (Fig 16) (56). Morphologic imaging studies such as CT and MR imaging are often insensitive compared with PET/CT for monitoring response after SIRT because of necrosis, edema, hemorrhage, and cystic change (56).

IGRT.—Imaging findings after targeted radiation therapy differ from those seen after percutaneous ablation or intra-arterial therapies. Treatment changes are seen in not only the targeted lesion but also in areas corresponding to the radiation zone. Jarraya et al (61) described CT features after targeted stereotactic body radiotherapy for liver malignancies and reported that the zone of irradiation appears as a sharply demarcated hypoattenuating area, with the lesion seen as a hypoattenuating area with peripheral rim enhancement. Successful treatment response is indicated by gradual shrinkage of the hypoattenuating lesion, while the surrounding hypoattenuating irradiated hepatic parenchyma gradually turns isoattenuating and then hyperattenuating (Fig 17) (61). Treatment failure is indicated by gradual increase in the size of the lesion, with lobulated, thick, heterogeneous enhancement of the irradiated tumor (61). At MR imaging, the liver parenchyma in the zone of radiation demonstrates well-demarcated areas of T1 hypointensity and slight T2 hyperintensity due to increased free water content in the zone of radiation compared with the surrounding hepatic parenchyma (62). T2 signal changes that are progressive and irreversible represent characteristic findings of radiation injury to the liver (62). Onaya et al (62) found that at dynamic gadolinium-enhanced MR imaging, irradiated areas demonstrated early, intense, prolonged enhancement that was more pronounced than in the surrounding normal liver parenchyma because of impeded drainage of blood caused

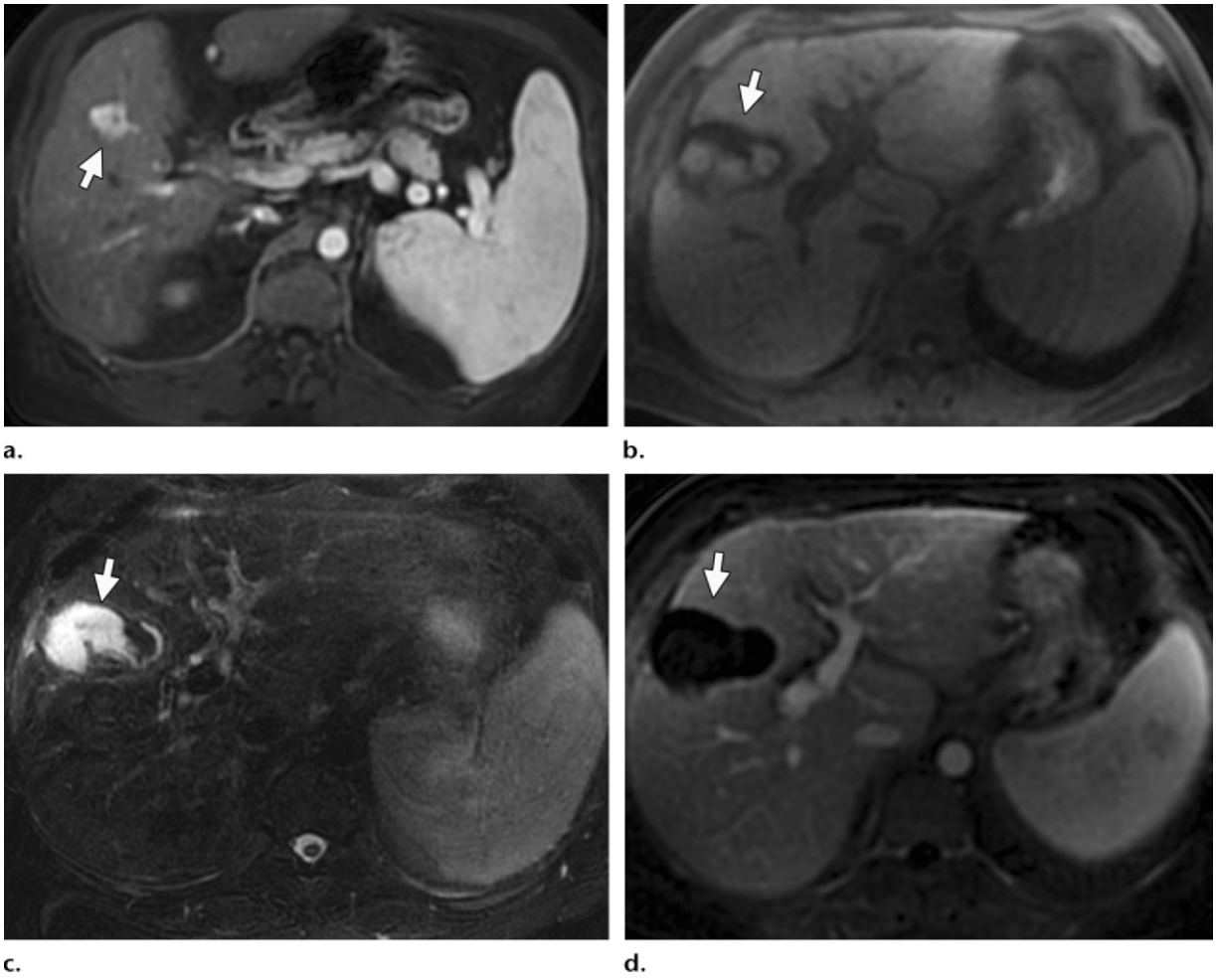

Figure 10. Expected changes seen at MR imaging after microwave ablation. **(a)** Axial gadolinium-enhanced pretreatment MR image shows an HCC (arrow) in liver segment 4. **(b, c)** Axial T1-weighted **(b)** and T2-weighted **(c)** MR images obtained 1 month after ablation show the ablation zone (arrow), with heterogeneous areas of hyperintensity seen in **b** and hypointensity seen in **c**. **(d)** Axial gadolinium-enhanced MR image shows no enhancement in the ablation zone (arrow) and a thin rim of peripheral enhancement, which are expected findings.

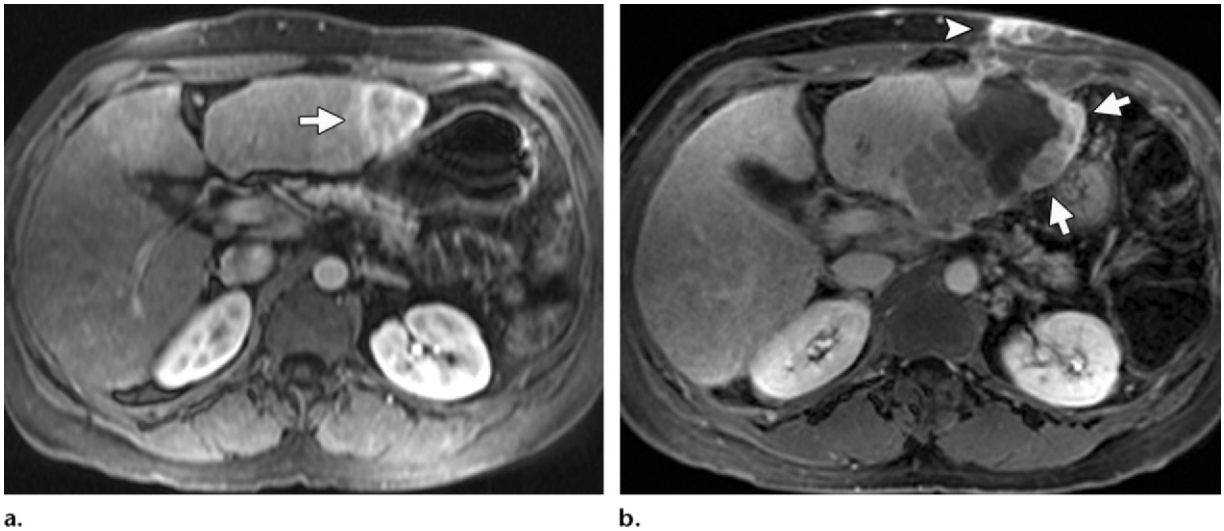

Figure 11. Abnormal imaging appearance after percutaneous ablation. **(a)** Axial gadolinium-enhanced pretreatment MR image shows a 3.4-cm HCC in the left lobe of the liver (arrow), a finding that was treated with RFA. **(b)** Axial gadolinium-enhanced MR image obtained 3 months after RFA shows nodular enhancement along the ablation zone (arrows), a finding suggestive of tumor recurrence. Note the enhancing areas in subcutaneous tissues in the ablation track (arrowhead). The findings were presumed to indicate tumor track seeding, but histologic confirmation could not be obtained.

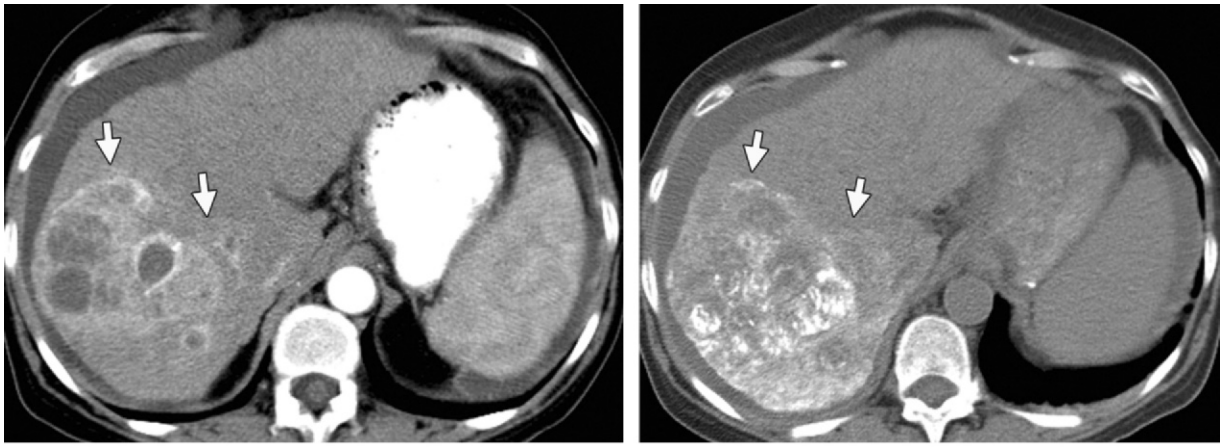

a. b.

Figure 12. Imaging appearance of HCC after TACE. **(a)** Axial contrast-enhanced pretreatment CT image shows a large, heterogeneous, arterially enhancing tumor (arrows) in the right hepatic lobe, a finding that was treated with iodized-oil TACE. **(b)** Axial nonenhanced CT image obtained 1 month after TACE shows dense deposition of iodized oil in the tumor (arrows).

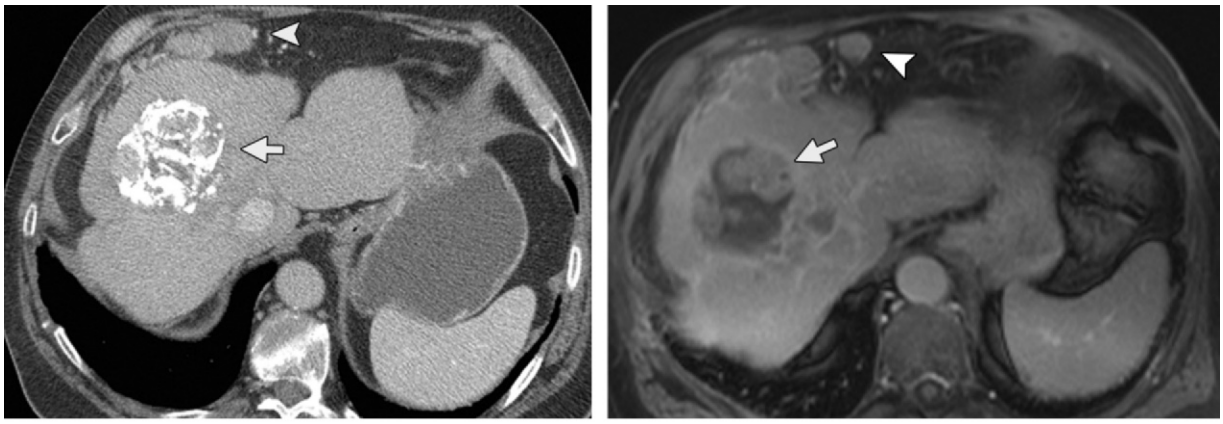

a. b.

Figure 13. MR imaging to determine tumor recurrence after TACE. **(a)** Axial contrast-enhanced CT image obtained after iodized-oil TACE of a dome HCC shows heterogeneous deposition of iodized oil in the tumor (arrow), a finding that limits assessment of enhancing tumor. Note the enlarged peridiaphragmatic and perihepatic lymph nodes (arrowhead in a and b) anterior to the liver, findings suggestive of lymph node metastases. **(b)** Axial gadolinium-enhanced MR image better depicts enhancing nodules in the tumor (arrow), findings suggestive of residual disease.

by hepatic venous obstruction due to radiation effects. Complete treatment response is indicated by total lack of tumor enhancement in the radiation zone. As with imaging findings after percutaneous ablation, a substantial decrease in tumor size might not be seen for several months after successful IGRT. Preliminary studies have shown that diffusion-weighted MR imaging is a valuable technique for monitoring response to radiation therapy, and early increase in the mean tumor ADC has been correlated with favorable response to radiation therapy (63).

Tumor Response Criteria

Conventionally established tumor metric systems such as World Health Organization criteria and Response Evaluation Criteria in Solid Tumors (RECIST), which are designed to evaluate tumor response to cytotoxic therapies that cause tumor shrinkage, are not well suited for monitoring response to local-regional therapies because these therapies often cause destruction or necrosis of targeted tumor tissue without size reduction (7). These criteria could even be misleading because image-guided therapies often lead to posttreatment stabilization or increase in tumor size despite satisfactory tumor destruction because of time lag between treatment and change in tumor dimensions (7). In addition, development of new hepatic or extrahepatic lesions after targeted therapy does not represent treatment failure but rather tumor progression.

To address these shortcomings, two new criteria, the European Association for the Study of the Liver (EASL) and Modified Response Evaluation Criteria in Solid Tumors (mRECIST),

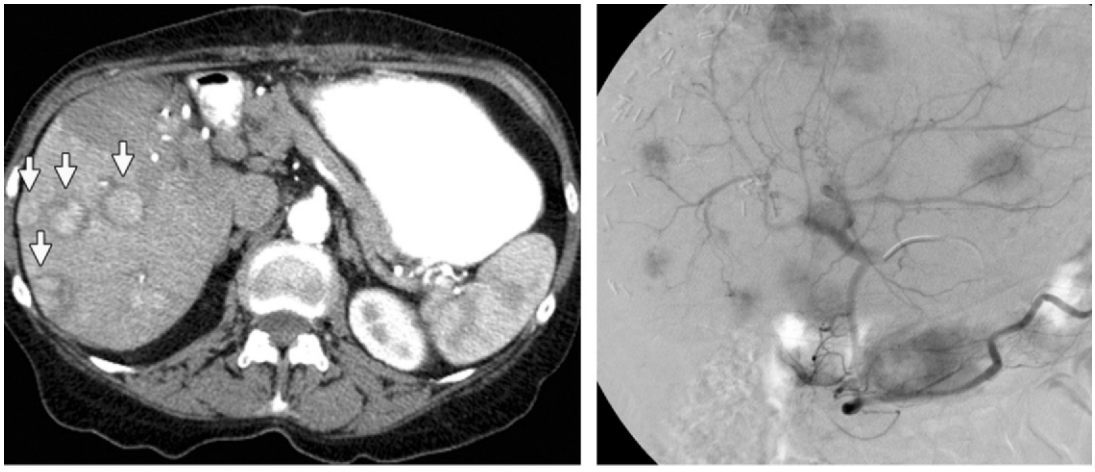

a. b.

c.

Figure 14. Multifocal recurrent HCC after TACE in a 70-year-old woman who previously underwent left hepatic trisegmentectomy for HCC. **(a)** Axial contrast-enhanced CT image obtained 6 months after trisegmentectomy shows multiple arterially enhancing HCCs (arrows) in the right hepatic lobe. Surgical clips from prior left hepatectomy are seen at the liver margins. **(b)** Digital subtraction angiographic spot image obtained during TACE shows selective cannulation of the hepatic artery, with multiple tumor blushes that correspond to the enhancing HCCs seen in **a**. **(c)** Axial contrast-enhanced CT image obtained 1 month after TACE shows treatment response suggested by absence of arterial enhancement in the tumors (arrows). No change in tumor size is seen.

were developed (Table 3). The basic principle of these criteria is that the most appropriate approach to treatment response evaluation is to estimate reduction in viable tumor dimensions at contrast-enhanced CT or gadolinium-enhanced MR imaging. Evaluation of reduced tumor load should include estimation of intratumoral necrotic areas and not mere decrease in overall tumor size (7). Viable tumor in the treatment zone manifests as enhancement at arterial phase CT or MR imaging of HCC (7) (Table 2). Arterial phase imaging is recommended because contrast between viable vascularized HCC and nonenhancing necrotic tissue is maximal in this phase (7). Measurements of viable tumor dimensions should be made without including intervening areas of tumor necrosis and need not be made in the same plane as measurement of baseline tumor diameter (7). Careful comparison of pre- and posttreatment images is essential to precisely identify enhancing and nonenhancing areas (7). Although these criteria were initially described for monitoring treatment response in HCCs, liver metastases treated with local-regional therapies can also be evaluated with these guidelines (7).

Advanced Imaging Methods

Postprocessing Techniques

Image Fusion.—Fusion of PET and CT images is routinely performed to combine anatomic details of CT with functional information of PET. In patients with hepatobiliary malignancies, the emerging role of PET/MR imaging will be particularly beneficial due to the superior soft-tissue resolution of MR imaging, which provides better lesion characterization than CT (Fig 18) (64). Advanced image fusion techniques are also increasingly used for accurate delivery of therapy to hepatobiliary tumors. For example, software-based fusion of US images with CT and MR images can be used to display synchronized CT or MR images in the same plane as US images for more accurate treatment guidance (64). Similarly, pre- and posttreatment fusion of CT and MR images can assist in evaluation of atttenuation and intensity changes at the treatment site (7).

Volumetric Methods.—Volumetric methods increasingly play a major role in evaluation of hepatobiliary malignancies before and after local-regional therapy. Semiautomated and automated segmentation methods allow estimation

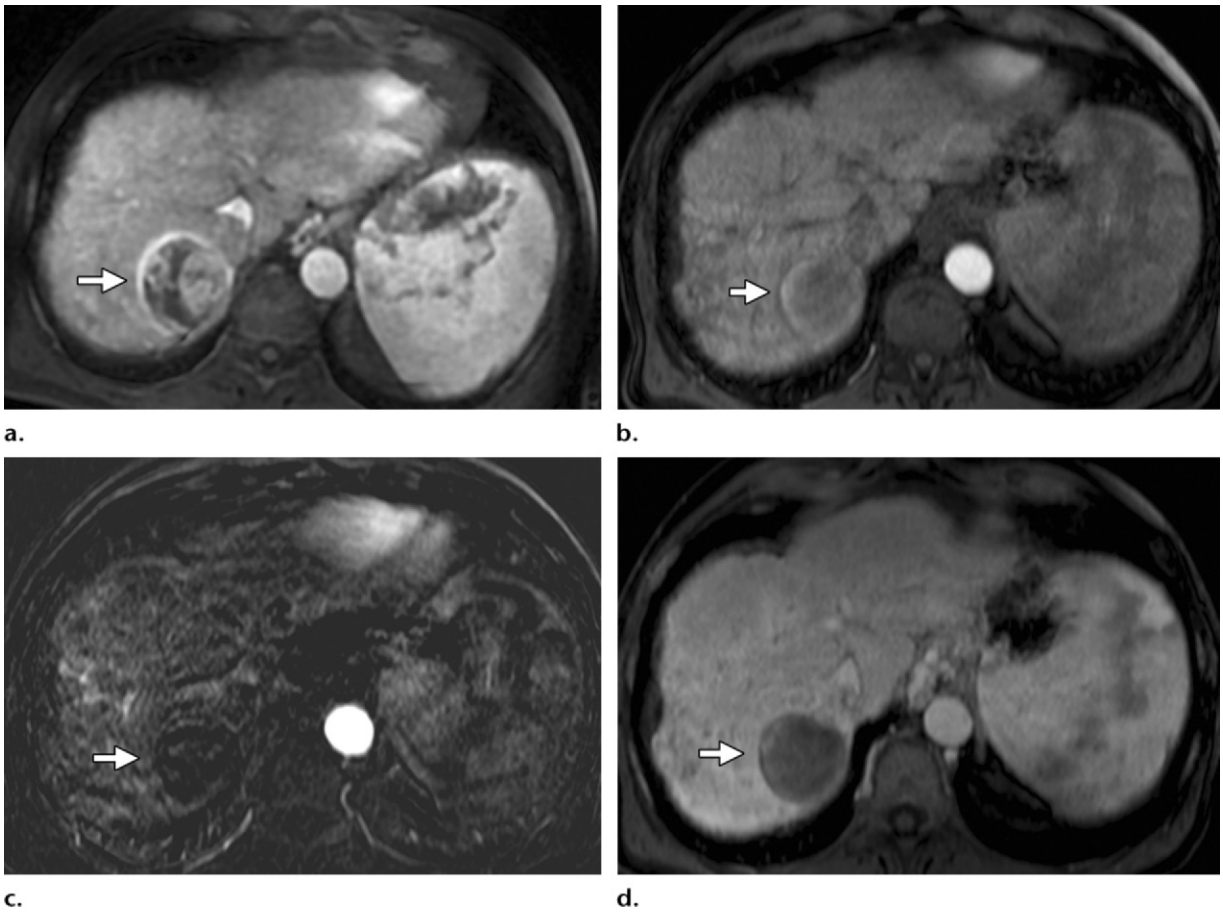

Figure 15. MR imaging after SIRT in a 66-year-old woman with cirrhosis. **(a)** Axial gadolinium-enhanced pretreatment MR image shows a heterogeneous arterially enhancing dome HCC (arrow). The patient underwent SIRT. **(b–d)** Axial gadolinium-enhanced arterial phase **(b)**, arterial phase subtraction **(c)**, and portal venous phase **(d)** MR images obtained 3 months after SIRT indicate complete tumor necrosis, suggested by lack of enhancement in the tumor (arrow).

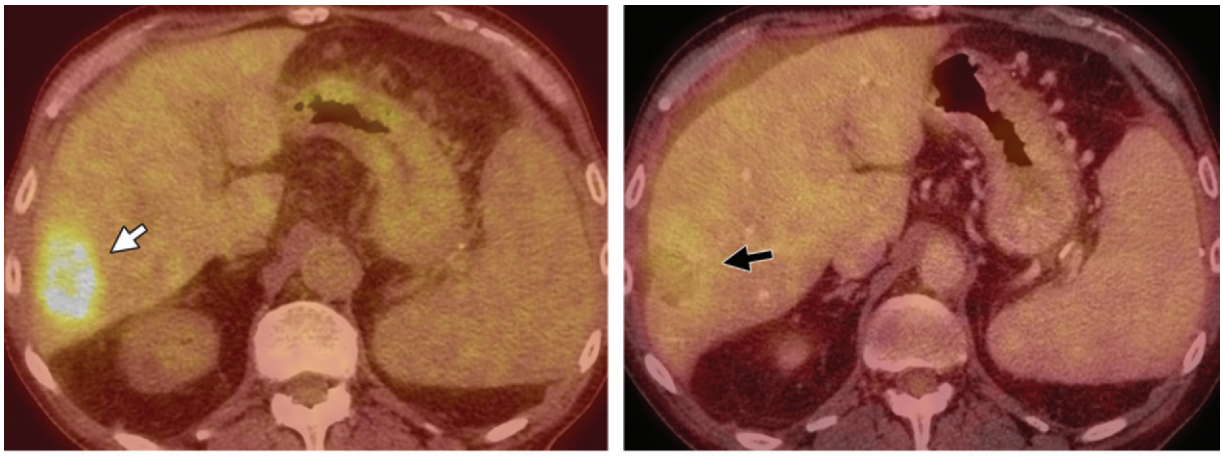

Figure 16. Fused PET/CT in a 53-year-old man after SIRT for liver metastases from colorectal cancer. **(a)** Fused PET/CT image obtained before SIRT shows a large, FDG-avid, metastatic deposit in the right lobe of the liver (arrow). **(b)** Fused PET/CT image obtained 3 months after SIRT shows no FDG avidity in the area (arrow), a finding indicative of complete response.

of tumor volume to plan liver-directed therapies. Volumetric liver assessment is indicated for evaluation of functional liver residue when major hepatic resection (> four segments) is planned or when there is underlying liver disease (29,51). In patients undergoing SIRT, estimation of liver tumor burden and liver volume is an essential component of pretreatment planning to calculate the treatment dose (^{90}Y) to limit toxic effects (Fig 19).

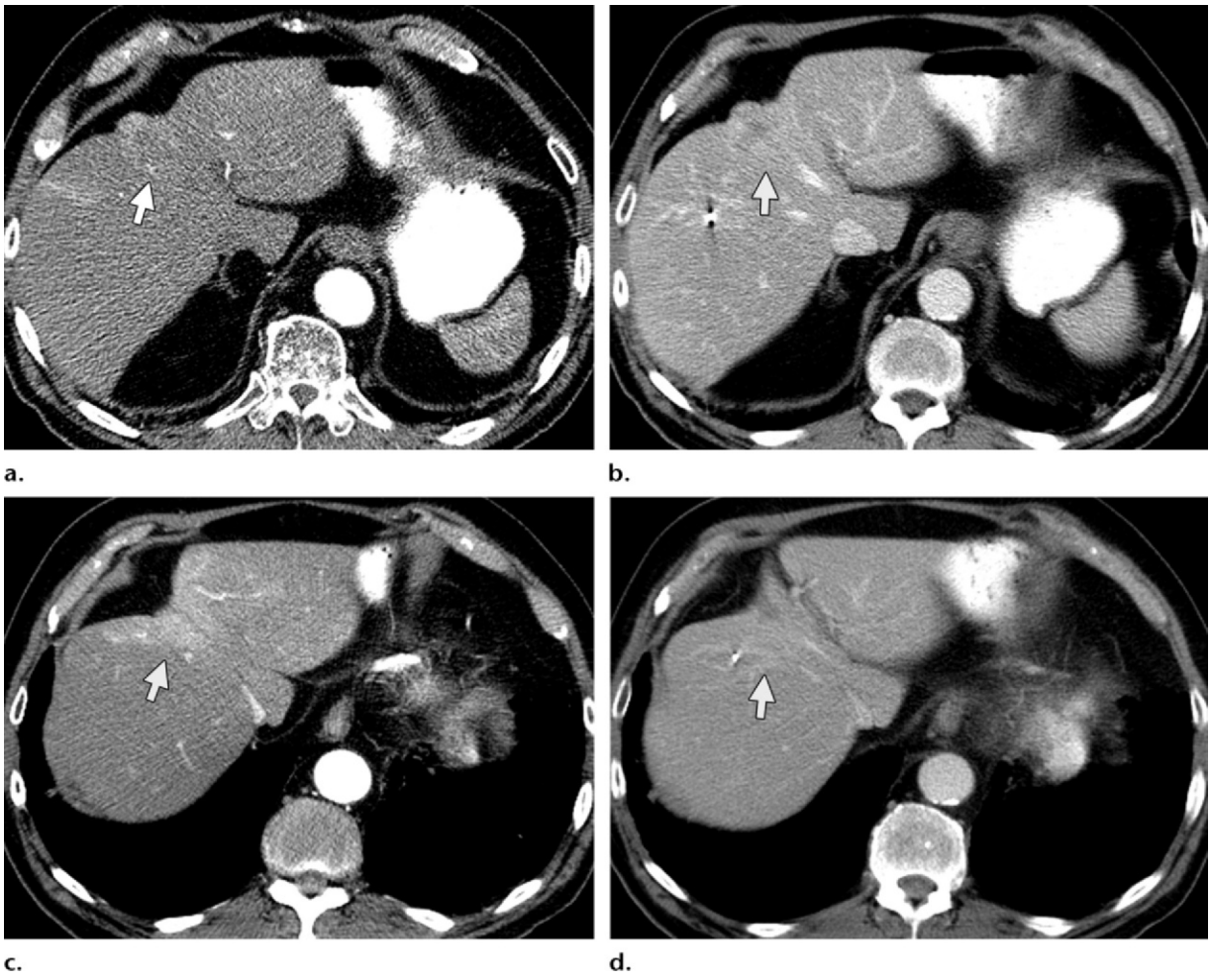

Figure 17. Proton beam therapy in an 84-year-old man with HCC. **(a, b)** Axial contrast-enhanced pretreatment CT images obtained in the arterial **(a)** and portal venous **(b)** phases show an arterially enhancing tumor (arrow) in segment 4 of the liver, with a washout appearance. **(c)** Axial contrast-enhanced arterial phase CT image obtained 6 months after proton beam therapy shows a well-demarcated radiation zone (arrow), with hyperenhancement and reduction in tumor size. **(d)** Axial contrast-enhanced portal venous phase CT image shows the hypoenhanced shrunken tumor (arrow).

Table 3: EASL and mRECIST Treatment Response Criteria for Local-Regional Therapies

	Response Criteria at Imaging	
Response Type	EASL	mRECIST
Complete response	Total disappearance of enhanced areas	Total disappearance of intratumoral areas of enhancement in arterial phase
Partial response	>50% decrease in enhanced areas	>30% decrease in sum of diameters of enhanced areas in arterial phase
Stable disease	Neither partial response nor progressive disease criteria met	Neither partial response nor progressive disease criteria met
Progressive disease	>25% increase in enhanced lesions	>20% increase in sum of diameters of enhanced areas in arterial phase

Two-dimensional morphologic tumor assessment methods that use CT and MR imaging have certain drawbacks in monitoring posttreatment response. These conventional methods assume that tumors have spherical dimensions, and they define the threshold for partial response as a 30% reduction in tumor diameter (presuming that this corresponds to a 65% reduction in tumor volume) (27). However, tumor volume estimates made with two-dimensional images are prone to interobserver variability and have been shown to differ from concurrent measurements made with three-dimensional images (27).

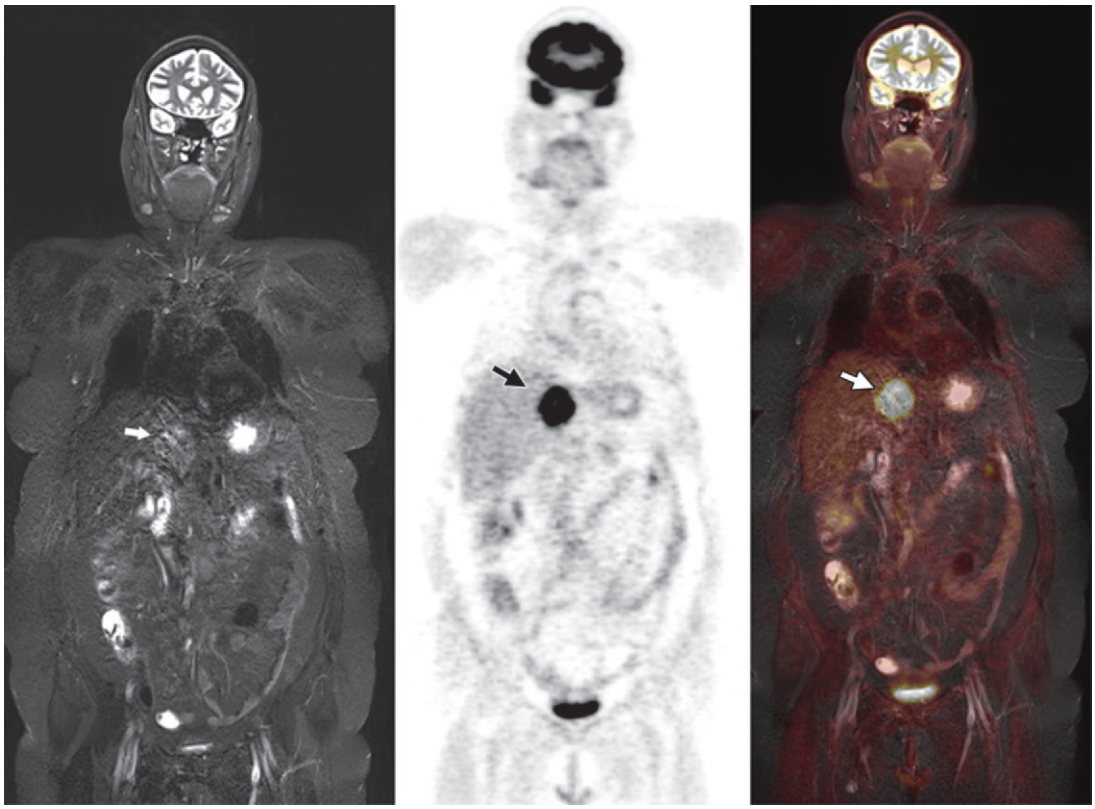

Figure 18. PET/MR image fusion in a 67-year-old man with a large left hepatic lobe metastasis from colorectal cancer. The lesion (arrows) appears slightly hyperintense on a T2-weighted MR image (left), with intense FDG avidity seen on PET (center) and PET/MR (right) images. The PET/MR fusion image accurately depicts the lesion's characteristics.

This is true for measurements of tumor diameter and estimates of the proportion of tumor necrosis (27). Volumetric evaluation of hepatic tumors eliminates this limitation and offers the most comprehensive means of anatomic assessment to determine treatment response (27). Studies have shown that volumetric increase in the ablation zone (compared with findings on initial postablation images) in patients with liver metastases from colorectal cancer is highly predictive of ablation zone tumor recurrence. Voxel-by-voxel volumetric analysis of tumor density and necrosis has been shown to be more precise and reproducible than two-dimensional measurements (27). This type of volumetric quantification is especially helpful and is a promising tool when necrosis is heterogeneously distributed in the tumor and cannot be accurately assessed with RECIST (27). Despite their utility, volumetric measurements have limited availability and have not been integrated into routine clinical practice (27).

Necrosis Quantification.—Directed therapies often affect tumor viability before changes in tumor size can be seen on images. Therefore, estimation of necrosis and viable tumor volume is a more sensitive biomarker for assessing success of local-regional therapies (27,65,66). Volumetric quantification of viable tumor tissue and necrosis is more accurate for determining response to local-regional therapies such as SIRT (Fig 20). Studies have shown that measurement of tumor necrosis allows earlier detection of response compared with World Health Organization criteria or RECIST in the early posttreatment phase after SIRT (67,68). Initial studies have demonstrated that measurements of tumor necrosis correlate with survival (67).

Dual-Energy CT.—Dual-energy CT is an exciting new technology that allows simultaneous acquisition of CT images by using different photon energies. Acquisition of data at two different energies (eg, 80 kVp and 140 kVp) provides opportunities for improved lesion detection and tissue characterization. The 80-kVp data and iodine-specific images generated at dual-energy CT have been shown to improve conspicuity of hypervascular liver lesions such as HCC and enhance detection of hypovascular metastases (Fig 21) (69–72). Depiction of hypovascular or hypoattenuating metastatic liver lesions is particularly improved on low-energy images in patients with diffuse fatty infiltration, which usually limits evaluation of liver metastases (71). Iodine maps or images obtained from dual-energy CT datasets provide critical information about distribution of iodine within the liver, which can be used to improve detection

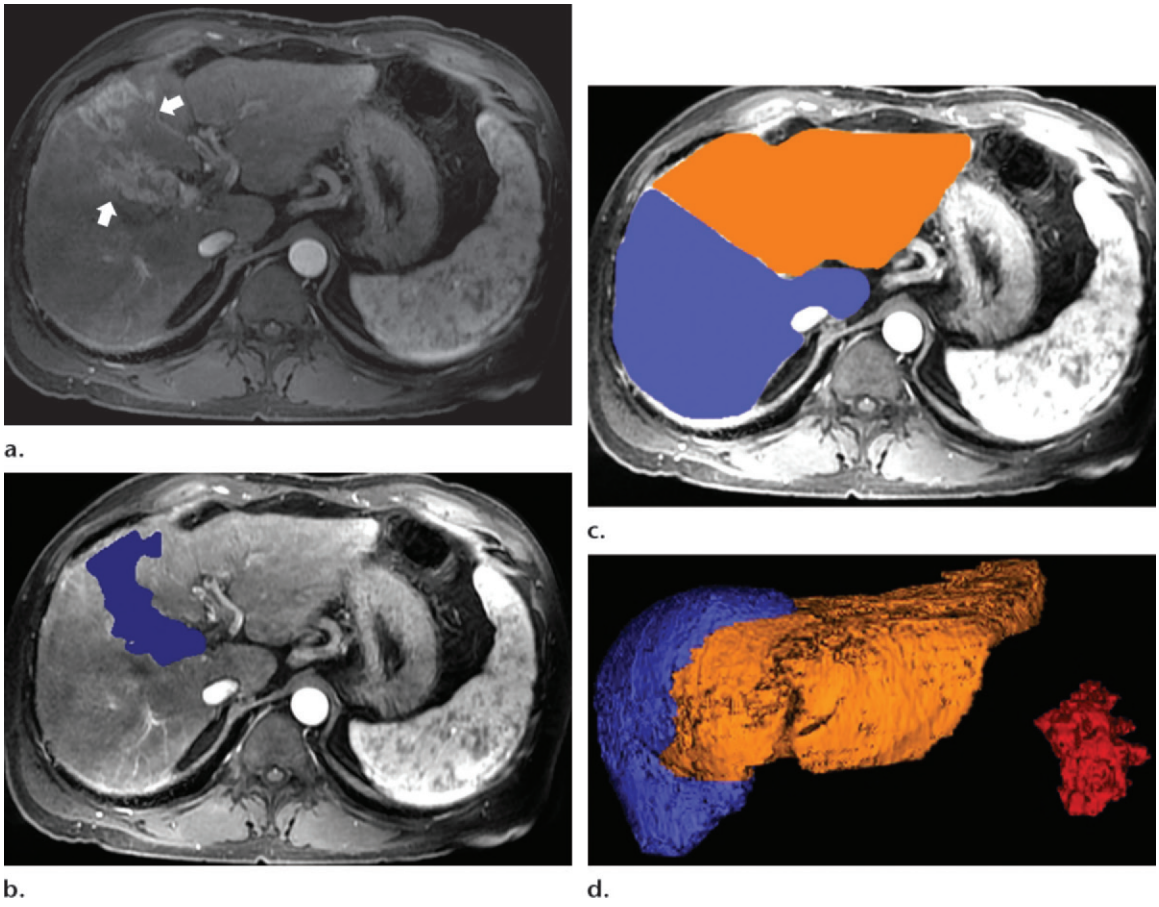

Figure 19. Volumetric assessment of hepatic tumor burden to determine treatment dose before SIRT. **(a)** Axial gadolinium-enhanced MR image shows a heterogeneously enhancing HCC in the liver (arrows). **(b)** Axial gadolinium-enhanced MR image with color overlay shows assessment of tumor volume (blue) with the segmentation method. **(c)** Axial MR image with color overlay shows the segmentation method used to measure liver volume. Blue = right lobe, orange = left lobe. **(d)** Volume-rendered MR images show the whole liver (blue = right lobe, orange = left lobe) and tumor (red).

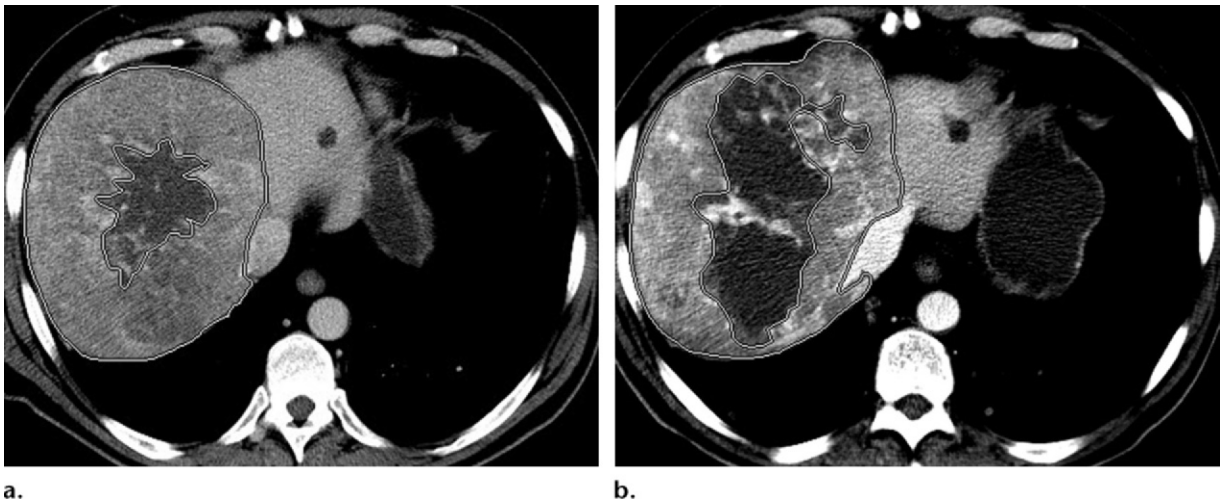

Figure 20. Volumetric assessment of tumor response to SIRT by necrosis quantification. The area between the two outlines represents enhancing viable tumor tissue. **(a)** Axial contrast-enhanced pretreatment CT image shows the region-of-interest segmentation method for necrosis quantification in a large HCC. **(b)** Axial contrast-enhanced CT image obtained after SIRT shows an increase in the tumor zone of necrosis.

of hypervascular liver masses (71). Low-energy monochromatic images generated at dual-energy CT also increase iodine conspicuity in the enhancing tumor and adjacent vasculature, thereby providing superior delineation of tumor margins and their relationship to adjacent vessels (71).

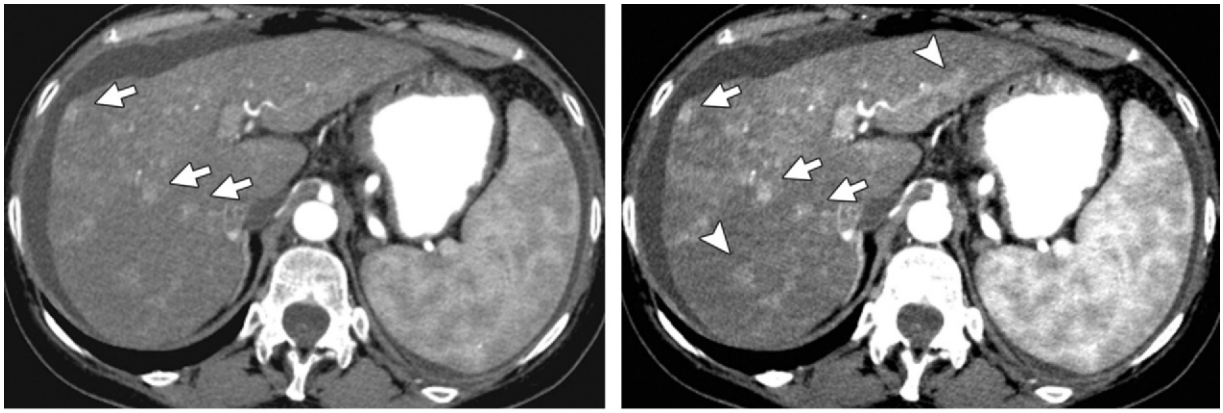

a. b.

Figure 21. Dual-energy CT for detection of hypervascular HCC in a 56-year-old woman with cirrhosis. **(a)** Axial contrast-enhanced arterial phase CT image shows multiple hypervascular liver lesions (arrows). **(b)** Axial postprocessed 50-keV CT image allows better visualization of the lesions (arrows) and identification of additional lesions (arrowheads) and improves diagnostic confidence.

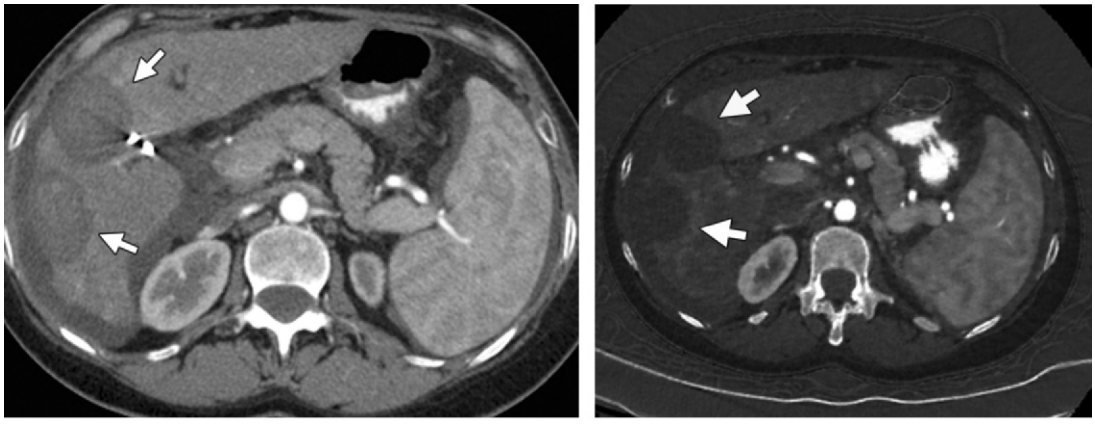

a. b.

Figure 22. Dual-energy CT to determine treatment response after RFA in a 56-year-old patient. **(a)** Contrast-enhanced arterial phase CT image obtained after RFA of two HCCs shows mild heterogeneity in the ablation zone (arrows). **(b)** Postprocessed iodine image shows no enhancement in the ablation zone (arrows), a finding indicative of successful ablation.

Routine CT evaluation after percutaneous ablation generally requires acquisition of nonenhanced and contrast-enhanced CT images, which are essential to accurately characterize abnormal enhancement in the ablation zone for early detection of residual or recurrent tumor. However, diagnosis of viable tumor in the heterogeneous ablation zone can be challenging because of hemorrhage, edema, and intralesional desiccation, which can be compounded by respiratory misregistration between nonenhanced and contrast-enhanced images (71). Qualitative and quantitative iodine maps obtained from postprocessed dual-energy CT datasets can enable more accurate detection of residual or recurrent tumor. Iodine maps and images allow precise determination of the distribution of iodine in the ablation zone and theoretically can improve detection of abnormal enhancement in the heterogeneous ablation zone and enhance detection of enhancing viable tumor after percutaneous ablation (73). Lee et al (73) showed that conspicuity of the internal characteristics of the ablation zone is improved on iodine maps versus regular CT images, which could improve detection of viable tumor in the ablation zone (Fig 22). Dual-energy CT–generated iodine maps can be used to evaluate and quantify tumor viability according to the amount of iodine seen in the lesions (71).

Perfusion CT or MR Imaging.—Tumor angiogenesis plays a crucial role in the pathophysiology of primary or secondary hepatic malignancies. Tumor vascular physiology is closely related to biologic aggressiveness of the tumor and thereby determines response to local and systemic therapies. Tumor vascularity can be evaluated at contrast-enhanced CT or MR imaging and transcatheter angiography. Perfusion CT or MR imaging is a functional imag-

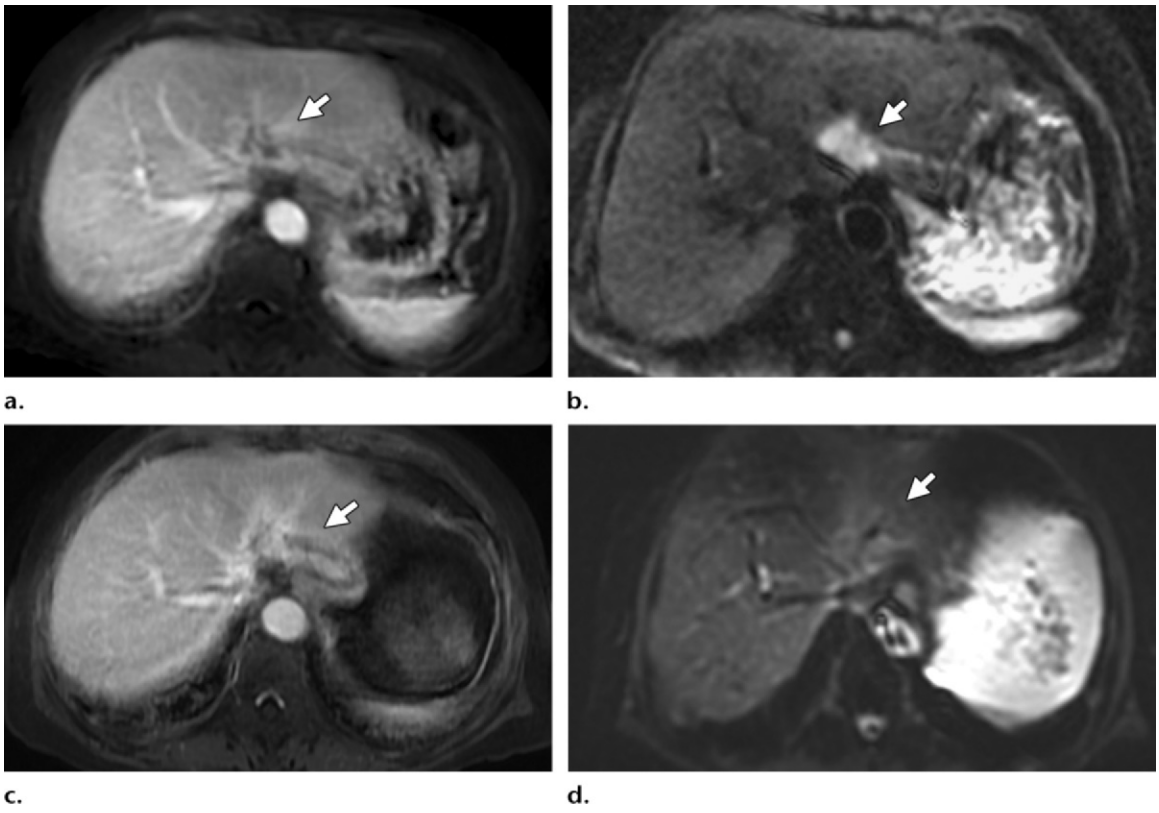

Figure 23. Diffusion-weighted imaging to assess treatment response after proton beam therapy for cholangiocarcinoma. **(a)** Axial gadolinium-enhanced portal venous phase pretreatment MR image shows a mass in the left lobe of the liver (arrow). **(b)** Axial diffusion-weighted pretreatment MR image (b = 600 sec/mm^2) shows restricted diffusion in the tumor (arrow). **(c)** Axial gadolinium-enhanced portal venous phase MR image obtained 6 months after IGRT shows heterogeneous tumor enhancement (arrow), which impedes accurate assessment of treatment response. **(d)** Corresponding diffusion-weighted MR image (b = 600 sec/mm^2) shows tumor hypointensity (arrow), a finding suggestive of treatment response.

ing tool that allows evaluation of tumor vascularity after serial image acquisition with administration of iodinated or gadolinium contrast material. Perfusion imaging has a potential role in evaluation of treatment response in patients with HCC after local-regional therapy. Perfusion imaging is performed in vivo, is noninvasive, and allows accurate estimation of tumor vascularity compared with morphologic methods (eg, size and density measurements). Disadvantages include limited availability and expertise and lack of standardized imaging protocols, analysis, and response criteria. Studies have shown that perfusion CT could be used to assess tumor response to intra-arterial therapies by demonstrating perfusion changes, and the results have validated the role of perfusion CT in quantification of residual viable tumor perfusion (74).

Functional MR Imaging Techniques.—Diffusion-weighted MR imaging is a functional imaging tool that permits quantitative and qualitative assessment of the mobility of water molecules in tissues and adds value to dynamic contrast-enhanced MR imaging. Diffusion-weighted MR imaging improves detection of liver metastases from colorectal cancer, particularly small (<1 cm) metastases that mimic intrahepatic vasculature, and highlights lesions close to the liver surface (75). The combination of diffusion-weighted and gadoxetic acid–enhanced MR imaging has also been shown to yield better diagnostic accuracy in detection of small HCCs (<2 cm) (76). Diffusion-weighted MR imaging is potentially helpful for monitoring tumor response after intra-arterial therapies because successfully treated tumors show increased ADCs due to increasing water diffusion after cellular destruction (7). Early changes in increased tissue diffusion at diffusion-weighted MR imaging after intra-arterial therapy have been shown to be a predictive biomarker for favorable outcomes or progression-free survival after TACE. Because of lag time between successful treatment and changes in tumor dimensions, diffusion-weighted MR imaging has been proposed as a superior technique for assessment of response after SIRT as early as 1 month after treatment in patients with HCC (7). After SIRT, necrotic tumor tissue demonstrates a significant increase in the mean ADC (7). Diffusion-weighted MR imaging after SIRT and IGRT might also help distinguish posttreatment inflammation from viable tumor (Fig 23) (7). Preliminary published reports on the value of diffusion-weighted imaging

in determination of local tumor progression after percutaneous RFA suggest that significant changes in ADC are not detected over time when the entire ablation zone is included in measurements (7). However, targeted evaluation of ADCs at the periphery of the ablation zone is useful to differentiate local tumor progression from inflammatory posttreatment changes, with recurrent tumors demonstrating lower ADCs (7).

Hydrogen 1 MR spectroscopy enables detection and quantification of tissue metabolite concentration. Hepatic tumors often show elevated choline concentration and choline-to-lipid ratios, and the metabolic signature can vary by tumor type and tumor aggressiveness. After local and systemic therapies, changes occur in the tumor metabolic spectrum, and MR spectroscopy can serve as an image biomarker for monitoring effects of local-regional therapies. Bian et al (77) reported that in patients with HCC treated with TACE, choline-to-lipid, glucogen- or glucose-to-lipid, and glytamine- or glutamate-to-lipid ratios were significantly different before and immediately after (3–10 days) TACE, which indicates that MR spectroscopy could be used to evaluate early metabolic response to TACE.

Complications

Imaging plays a crucial role in evaluation of complications after local-regional therapies. Early identification of posttreatment complications is essential for immediate intervention. Complications after percutaneous ablation include hemorrhage, infection, pneumothorax, pleural effusion, hepatic insufficiency, arteriovenous fistula, biloma, and biliary stricture formation (Fig 4). Tumor seeding is a rare complication of ablation, is seen as enhancing tissue along the ablation track, and must be differentiated from inflammatory response or infective complications. Complications of intra-arterial therapies include biliary disease (biliary necrosis, stricture, and cholecystitis; <10% of patients), hepatic disease (early complications: transaminitis, acute liver failure; late complications: fibrosis or cirrhosis with ascites, portal hypertension; 0%–4% of patients), radiation pneumonitis (< 1%), access site injuries (hematoma), hepatic artery injury (dissection, thrombosis), nontarget embolization, infection (hepatic abscess), biliary strictures or biloma, and hepatic failure.

Conclusion

Imaging is crucial to successful management of hepatobiliary tumors with use of novel targeted therapies. Knowledge of the role of imaging in pretreatment planning, therapy guidance, and posttreatment evaluation is essential for optimal treatment results. Recognition and differentiation of normal posttreatment changes from residual or recurrent disease is necessary to prevent identification of benign changes as abnormal findings, which could result in needless additional interventions.

***Disclosures of Conflicts of Interest.*—A.R.G.** *Activities related to the present article:* disclosed no relevant relationships. *Activities not related to the present article:* speaker for Siemens Medical Solutions; expert witness for Rice, Dolan, and Kershaw. *Other activities:* disclosed no relevant relationships. **D.S.** *Activities related to the present article:* disclosed no relevant relationships. *Activities not related to the present article:* royalties from Elsevier. *Other activities:* disclosed no relevant relationships.

References

1. Adam R, De Gramont A, Figueras J, et al. The oncosurgery approach to managing liver metastases from colorectal cancer: a multidisciplinary international consensus. Oncologist 2012;17(10):1225–1239.
2. Bruix J, Sherman M; Practice Guidelines Committee, American Association for the Study of Liver Diseases. Management of hepatocellular carcinoma. Hepatology 2005;42(5):1208–1236.
3. Bruix J, Sherman M, Llovet JM, et al, for the EASL Panel of Experts on HCC. Clinical management of hepatocellular carcinoma: conclusions of the Barcelona-2000 EASL conference. J Hepatol 2001;35(3):421–430.
4. Fisher RA, Maluf DG, Wolfe L, et al. Is hepatic transplantation justified for primary liver cancer? J Surg Oncol 2007;95(8):674–679.
5. Fisher RA, Maroney TP, Fulcher AS, et al. Hepatocellular carcinoma: strategy for optimizing surgical resection, transplantation and palliation. Clin Transplant 2002;16(suppl 7): S52–S58.
6. Mahnken AH, Pereira PL, de Baère T. Interventional oncologic approaches to liver metastases. Radiology 2013;266(2):407–430.
7. Crocetti L, Della Pina C, Cioni D, Lencioni R. Peri-intraprocedural imaging: US, CT, and MRI. Abdom Imaging 2011;36(6):648–660.
8. Crocetti L, Lencioni R. Thermal ablation of hepatocellular carcinoma. Cancer Imaging 2008;8:19–26.
9. Gervais DA, Goldberg SN, Brown DB, Soulen MC, Millward SF, Rajan DK. Society of Interventional Radiology position statement on percutaneous radiofrequency ablation for the treatment of liver tumors. J Vasc Interv Radiol 2009; 20(suppl 7):S342–S347.
10. Molla N, AlMenieir N, Simoneau E, et al. The role of interventional radiology in the management of hepatocellular carcinoma. Curr Oncol 2014;21(3):e480–e492.
11. Tsochatzis EA, Germani G, Burroughs AK. Transarterial chemoembolization, transarterial chemotherapy, and intra-arterial chemotherapy for hepatocellular carcinoma treatment. Semin Oncol 2010;37(2):89–93.
12. Wang N, Guan Q, Wang K, et al. TACE combined with PEI versus TACE alone in the treatment of HCC: a meta-analysis. Med Oncol 2011;28(4):1038–1043.
13. Kalva SP, Thabet A, Wicky S. Recent advances in transarterial therapy of primary and secondary liver malignancies. RadioGraphics 2008;28(1):101–117.
14. Kambadakone AR, Ganguli S, Mueller PR. Interventional radiology in the management of hepatocellular carcinoma in liver cirrhosis. Ann Gastroenterol Hepatol (Paris) 2011; 2(1):1–12.
15. Bester L, Meteling B, Boshell D, Chua TC, Morris DL. Transarterial chemoembolisation and radioembolisation for the treatment of primary liver cancer and secondary liver cancer: a review of the literature. J Med Imaging Radiat Oncol 2014;58(3):341–352.
16. Park HC, Seong J, Tanaka M, et al. Multidisciplinary management of nonresectable hepatocellular carcinoma. Oncology 2011;81(suppl 1):S134–S140.

17. Park HJ, Kim SH, Jang KM, et al. Added value of diffusion-weighted MRI for evaluating viable tumor of hepatocellular carcinomas treated with radiotherapy in patients with chronic liver disease. AJR Am J Roentgenol 2014;202(1):92–101.
18. Korean Liver Cancer Study Group and National Cancer Center, Korea. Practice guidelines for management of hepatocellular carcinoma 2009 [in Korean]. Korean J Hepatol 2009;15(3):391–423.
19. Kim M, Son SH, Won YK, Kay CS. Stereotactic ablative radiotherapy for oligometastatic disease in liver. Biomed Res Int 2014;2014:340478.
20. Swaminath A, Dawson LA. Emerging role of radiotherapy in the management of liver metastases. Cancer J 2010;16(2):150–155.
21. Hur H, Ko YT, Min BS, et al. Comparative study of resection and radiofrequency ablation in the treatment of solitary colorectal liver metastases. Am J Surg 2009;197(6):728–736.
22. Ong SL, Gravante G, Metcalfe MS, Strickland AD, Dennison AR, Lloyd DM. Efficacy and safety of microwave ablation for primary and secondary liver malignancies: a systematic review. Eur J Gastroenterol Hepatol 2009; 21(6):599–605.
23. Brock KK. Imaging and image-guided radiation therapy in liver cancer. Semin Radiat Oncol 2011;21(4):247–255.
24. Riaz A, Kulik LM, Mulcahy MF, Lewandowski RJ, Salem R. Yttrium-90 radioembolization in the management of liver malignancies. Semin Oncol 2010;37(2):94–101.
25. Ursino S, Greco C, Cartei F, et al. Radiotherapy and hepatocellular carcinoma: update and review of the literature. Eur Rev Med Pharmacol Sci 2012;16(11):1599–1604.
26. Schima W, Ba-Ssalamah A, Kurtaran A, Schindl M, Gruenberger T. Post-treatment imaging of liver tumours. Cancer Imaging 2007;7(Spec No A):S28–S36.
27. Yaghmai V, Besa C, Kim E, Gatlin JL, Siddiqui NA, Taouli B. Imaging assessment of hepatocellular carcinoma response to locoregional and systemic therapy. AJR Am J Roentgenol 2013;201(1):80–96.
28. Boonsirikamchai P, Loyer EM, Choi H, Charnsangavej C. Planning and follow-up after ablation of hepatic tumors: imaging evaluation. Surg Oncol Clin N Am 2011;20(2):301–315, viii.
29. Vauthey JN, Dixon E, Abdalla EK, et al. Pretreatment assessment of hepatocellular carcinoma: expert consensus statement. HPB (Oxford) 2010;12(5):289–299.
30. Bouza C, López-Cuadrado T, Alcázar R, Saz-Parkinson Z, Amate JM. Meta-analysis of percutaneous radiofrequency ablation versus ethanol injection in hepatocellular carcinoma. BMC Gastroenterol 2009;9:31.
31. Lencioni R, Cioni D, Della Pina C, Crocetti L. Hepatocellular carcinoma: new options for image-guided ablation. J Hepatobiliary Pancreat Sci 2010;17(4):399–403.
32. Lencioni R, Crocetti L, Pina MC, Cioni D. Percutaneous image-guided radiofrequency ablation of liver tumors. Abdom Imaging 2009;34(5):547–556.
33. Liang P, Wang Y. Microwave ablation of hepatocellular carcinoma. Oncology 2007;72(suppl 1):124–131.
34. Narayanan G, Hosein PJ, Arora G, et al. Percutaneous irreversible electroporation for downstaging and control of unresectable pancreatic adenocarcinoma. J Vasc Interv Radiol 2012;23(12):1613–1621.
35. Kim YS, Rhim H, Lim HK, et al. Intraoperative radiofrequency ablation for hepatocellular carcinoma: long-term results in a large series. Ann Surg Oncol 2008;15(7):1862–1870.
36. Livraghi T, Goldberg SN, Lazzaroni S, Meloni F, Solbiati L, Gazelle GS. Small hepatocellular carcinoma: treatment with radio-frequency ablation versus ethanol injection. Radiology 1999;210(3):655–661.
37. Clasen S, Boss A, Schmidt D, et al. Magnetic resonance imaging for hepatic radiofrequency ablation. Eur J Radiol 2006;59(2):140–148.
38. Donati OF, Fischer MA, Chuck N, Hunziker R, Weishaupt D, Reiner CS. Accuracy and confidence of Gd-EOB-DTPA enhanced MRI and diffusion-weighted imaging alone and in combination for the diagnosis of liver metastases. Eur J Radiol 2013;82(5):822–828.
39. Haimerl M, Wächtler M, Platzek I, et al. Added value of Gd-EOB-DTPA-enhanced hepatobiliary phase MR imaging in evaluation of focal solid hepatic lesions. BMC Med Imaging 2013;13:41.
40. Chen L, Zhang L, Bao J, et al. Comparison of MRI with liver-specific contrast agents and multidetector row CT for the detection of hepatocellular carcinoma: a meta-analysis of 15 direct comparative studies. Gut 2013;62(10):1520–1521.
41. Scharitzer M, Ba-Ssalamah A, Ringl H, et al. Preoperative evaluation of colorectal liver metastases: comparison between gadoxetic acid-enhanced 3.0-T MRI and contrast-enhanced MDCT with histopathological correlation. Eur Radiol 2013;23(8):2187–2196.
42. Jeong HT, Kim MJ, Park MS, et al. Detection of liver metastases using gadoxetic-enhanced dynamic and 10- and 20-minute delayed phase MR imaging. J Magn Reson Imaging 2012;35(3):635–643.
43. Lafaro KJ, Roumanis P, Demirjian AN, Lall C, Imagawa DK. Gd-EOB-DTPA–enhanced MRI for detection of liver metastases from colorectal cancer: a surgeon's perspective! Int J Hepatol 2013;2013:572307.
44. Halavaara J, Breuer J, Ayuso C, et al. Liver tumor characterization: comparison between liver-specific gadoxetic acid disodium–enhanced MRI and biphasic CT: a multicenter trial. J Comput Assist Tomogr 2006;30(3):345–354.
45. Hammerstingl R, Huppertz A, Breuer J, et al. Diagnostic efficacy of gadoxetic acid (Primovist)-enhanced MRI and spiral CT for a therapeutic strategy: comparison with intraoperative and histopathologic findings in focal liver lesions. Eur Radiol 2008;18(3):457–467.
46. Gervais DA, Goldberg SN, Brown DB, et al. Society of Interventional Radiology position statement on percutaneous radiofrequency ablation for the treatment of liver tumors. J Vasc Interv Radiol 2009;20(1):3–8.
47. Brennan IM, Ahmed M. Imaging features following transarterial chemoembolization and radiofrequency ablation of hepatocellular carcinoma. Semin Ultrasound CT MR 2013;34(4):336–351.
48. Crocetti L, de Baere T, Lencioni R. Quality improvement guidelines for radiofrequency ablation of liver tumours. Cardiovasc Intervent Radiol 2010;33(1):11–17.
49. Hompes D, Prevoo W, Ruers T. Radiofrequency ablation as a treatment tool for liver metastases of colorectal origin. Cancer Imaging 2011;11:23–30.
50. Arellano RS, Garcia RG, Gervais DA, Mueller PR. Percutaneous CT-guided radiofrequency ablation of renal cell carcinoma: efficacy of organ displacement by injection of 5% dextrose in water into the retroperitoneum. AJR Am J Roentgenol 2009;193(6):1686–1690.
51. Guenette JP, Dupuy DE. Radiofrequency ablation of colorectal hepatic metastases. J Surg Oncol 2010;102(8): 978–987.
52. de Baere T, Deschamps F, Briggs P, et al. Hepatic malignancies: percutaneous radiofrequency ablation during percutaneous portal or hepatic vein occlusion. Radiology 2008;248(3):1056–1066.
53. Hedgire SS, Elmi A, Kambadakone AR, Yoon S, Blake M, Harisinghani MG. MDCT imaging of Alloderm biologic mesh spacers in the abdomen and pelvis: preliminary experience. Clin Imaging 2014;38(3):279–282.
54. Yoon SS, Chen YL, Kambadakone A, Schmidt B, Delaney TF. Surgical placement of biologic mesh spacers prior to external beam radiation for retroperitoneal and pelvic tumors. Pract Radiat Oncol 2013;3(3):199–208.
55. Catalano OA, Choy G, Zhu A, Hahn PF, Sahani DV. Differentiation of malignant thrombus from bland thrombus of the portal vein in patients with hepatocellular carcinoma: application of diffusion-weighted MR imaging. Radiology 2010;254(1):154–162.
56. Dierckx R, Maes A, Peeters M, Van De Wiele C. FDG PET for monitoring response to local and locoregional therapy in HCC and liver metastases. Q J Nucl Med Mol Imaging 2009;53(3):336–342.
57. Sahani DV, Bajwa MA, Andrabi Y, Bajpai S, Cusack JC. Current status of imaging and emerging techniques to

evaluate liver metastases from colorectal carcinoma. Ann Surg 2014;259(5):861–872.
58. Kloeckner R, Otto G, Biesterfeld S, Oberholzer K, Dueber C, Pitton MB. MDCT versus MRI assessment of tumor response after transarterial chemoembolization for the treatment of hepatocellular carcinoma. Cardiovasc Intervent Radiol 2010;33(3):532–540.
59. Kubota K, Hisa N, Nishikawa T, et al. Evaluation of hepatocellular carcinoma after treatment with transcatheter arterial chemoembolization: comparison of Lipiodol-CT, power Doppler sonography, and dynamic MRI. Abdom Imaging 2001;26(2):184–190.
60. Zytoon AA, Ishii H, Murakami K, et al. Recurrence-free survival after radiofrequency ablation of hepatocellular carcinoma: a registry report of the impact of risk factors on outcome. Jpn J Clin Oncol 2007;37(9):658–672.
61. Jarraya H, Mirabel X, Taieb S, et al. Image-based response assessment of liver metastases following stereotactic body radiotherapy with respiratory tracking. Radiat Oncol 2013; 8:24.
62. Onaya H, Itai Y, Yoshioka H, et al. Changes in the liver parenchyma after proton beam radiotherapy: evaluation with MR imaging. Magn Reson Imaging 2000;18(6):707–714.
63. Eccles CL, Haider EA, Haider MA, Fung S, Lockwood G, Dawson LA. Change in diffusion weighted MRI during liver cancer radiotherapy: preliminary observations. Acta Oncol 2009;48(7):1034–1043.
64. Giesel FL, Mehndiratta A, Locklin J, et al. Image fusion using CT, MRI and PET for treatment planning, navigation and follow up in percutaneous RFA. Exp Oncol 2009;31 (2):106–114.
65. Chalian H, Tochetto SM, Töre HG, Rezai P, Yaghmai V. Hepatic tumors: region-of-interest versus volumetric analysis for quantification of attenuation at CT. Radiology 2012;262(3):853–861.
66. Galizia MS, Töre HG, Chalian H, McCarthy R, Salem R, Yaghmai V. MDCT necrosis quantification in the assessment of hepatocellular carcinoma response to yttrium 90 radioembolization therapy: comparison of two-dimensional and volumetric techniques. Acad Radiol 2012;19(1):48–54.
67. Monsky WL, Garza AS, Kim I, et al. Treatment planning and volumetric response assessment for yttrium-90 radioembolization: semiautomated determination of liver volume and volume of tumor necrosis in patients with hepatic malignancy. Cardiovasc Intervent Radiol 2011;34(2):306–318.
68. Miller FH, Keppke AL, Reddy D, et al. Response of liver metastases after treatment with yttrium-90 microspheres: role of size, necrosis, and PET. AJR Am J Roentgenol 2007;188(3):776–783.
69. Kim KS, Lee JM, Kim SH, et al. Image fusion in dual energy computed tomography for detection of hypervascular liver hepatocellular carcinoma: phantom and preliminary studies. Invest Radiol 2010;45(3):149–157.
70. Altenbernd J, Heusner TA, Ringelstein A, Ladd SC, Forsting M, Antoch G. Dual-energy-CT of hypervascular liver lesions in patients with HCC: investigation of image quality and sensitivity. Eur Radiol 2011;21(4):738–743.
71. Agrawal MD, Pinho DF, Kulkarni NM, Hahn PF, Guimaraes AR, Sahani DV. Oncologic applications of dual-energy CT in the abdomen. RadioGraphics 2014;34(3):589–612.
72. Robinson E, Babb J, Chandarana H, Macari M. Dual source dual energy MDCT: comparison of 80 kVp and weighted average 120 kVp data for conspicuity of hypo-vascular liver metastases. Invest Radiol 2010;45(7):413–418.
73. Lee SH, Lee JM, Kim KW, et al. Dual-energy computed tomography to assess tumor response to hepatic radiofrequency ablation: potential diagnostic value of virtual noncontrast images and iodine maps. Invest Radiol 2011; 46(2):77–84.
74. Ippolito D, Bonaffini PA, Ratti L, et al. Hepatocellular carcinoma treated with transarterial chemoembolization: dynamic perfusion-CT in the assessment of residual tumor. World J Gastroenterol 2010;16(47):5993–6000.
75. Chandarana H, Taouli B. Diffusion and perfusion imaging of the liver. Eur J Radiol 2010;76(3):348–358.
76. Park MJ, Kim YK, Lee MW, et al. Small hepatocellular carcinomas: improved sensitivity by combining gadoxetic acid–enhanced and diffusion-weighted MR imaging patterns. Radiology 2012;264(3):761–770.
77. Bian DJ, Xiao EH, Hu DX, et al. Magnetic resonance spectroscopy on hepatocellular carcinoma after transcatheter arterial chemoembolization. Chin J Cancer 2010;29(2):198–201.